SYNTHESIS AND BIOLOGICAL SCREENING OF SOME PYRAZOLE DERIVATIVES AS ANTIMALARIAL AND ANTILEISHMANIAL AGENTS

ADDIS ABABA UNIVERSITY

SCHOOL OF PHARMACY

DEPARTMENT OF PHARMACEUTICAL CHEMISTRY AND PHARMACOGNOSY

BY

ABDU TUHA

ADVISOR: PROFESSOR ADNAN A. BEKHIT (Ph.D)

June, 2012

SYNTHESIS AND BIOLOGICAL SCREENING OF SOME PYRAZOLE DERIVATIVES AS ANTIMALARIAL AND ANTILEISHMANIAL AGENTS

A thesis submitted to the School of Graduate Studies of Addis Ababa University in partial fulfillment of the requirements for the Degree of Master of Science in Medicinal Chemistry.

By

ABDU TUHA

Under the supervision of

Prof. Adnan A. Bekhit, Ph.D.

June 2012

Acknowledgment

All praise is to **ALLAH**, the lord of the universe and the Hereafter for his bounty upon to me. Peace be upon His Messenger.

My sincere thanks and gratitude goes to my advisor **Prof. Adnan A. Bekhit** for his indispensable advice, continuous moral, intellectual and material support. Special gratitude is due also to **Dr. Ariaya Hymete** for the valuable advice and scholastic revision and proof-reading of this work.

My appreciation also goes to the Egyptian Fund for technical cooperation with Africa, Ministry of foreign affairs, Egypt. I am also grateful to Department of Pharmaceutical Chemistry, Faculty of Pharmacy, Alexandria University for providing chemicals, and conducting the anti-leishmanial activity test and elemental microanalysis.

Special thank also goes to Wollo University for granting me this scholarship and Addis Ababa University for financially supporting this thesis work.

My heartfelt gratitude is due to my family for their love and moral support; may Allah pay you all.

Lastly, all friends are gratefully acknowledged for their advice and support that was of great value for this work and my overall academic performance.

Table of contents

Content

Acknowledgment i
List of tables vi
Abstract viii
1. INTRODUCTION 1
1.1 Background on malaria 1
1.1.1 Malaria Prevalence and its consequences 2
1.1.2 Life cycle of malaria 5
1.1.3 Drug targets for antimalarial treatment 6
1.1.3.1 Nucleic acid inhibitors 7
1.1.3.1.1 Folate antagonists 7
1. 1.3.1.2 DHODase blockers 7
1.1.3.2 Blood schizontocides 8
1.1.3.2.1 Haem disposal 8
1.1.3.2.2 Free radical formation 9
1.1.4 Novel molecular targets 9
1.1.4.1 Parasite membrane biosynthesis 9
1.1.4.2 Parasite transporters 10
1.1.4.3 Parasite proteases 10
1.1.4.4 The redox system 11
1.1.5 Drugs currently used against malaria 11
1.1.6 Antimalarial drug resistance 12
1.2 Background on leishmaniasis 13
1.2.1 Epidemiology of leishmaniasis 14
1.2.2 Life cycle of leishmania parasite 15
1.2.3 Drugs available for treatment of leishmaniasis 16
1.3 Pyrazole derivatives as biologically active compounds 17
1.4 Reported methods for synthesis of pyrazole chalcones 21
2. OBJECTIVES 25
2.1 General objective 25
2.2 Specific objectives 25
3. EXPERIMENTAL 25
3.1 Materials Used 25

3.1.1 Chemicals and Reagents 25
3.1.2 Instruments and apparatus 26
3.1.3 Experimental animals and parasite strain 27
3.1.4 Standard Drugs 27
3.2 Methods 28
3.2.1 Synthesis of target compounds 28
3.2.2 Determination of physical constants for synthesized compounds 32
3.2.3 Spectroscopic analysis of synthesized compounds 33
3.2.3.1 IR analysis 33
3.2.3.2 ^{1}H NMR analysis 33
3.2.4 Culture conditions 33
3.2.5 Stock solution and working concentration preparation 33
3.2.6 Biological activity test 34
3.2.6.1 *In vivo* antimalarial activity test 34
3.2.6.2 *In vitro* antipromastigote assay 35
3.2.7 Data analysis 37
4 RESULTS AND DISCUSSION 38
4.1 Synthesis of target compounds 38
4.1.1 Synthesis of the intermediate compound 38
4.1.2 Synthesis of thienyl and phenyl pyrazoline derivatives 39
4.2 Physical properties, percentage yield and elemental microanalysis 39
4.3 Spectral analysis of synthesized compounds. 41
4.4 Biological assays 68
4.4.1 *In vivo* antimalarial activity 68
4.4.2 *In vitro* antipromastigote activity 69
5 CONCLUSION 72
6 RECOMMENDATION 73
7 REFERENCES 74

List of figures

Figure 1: Life cycle of malaria parasite, plasmodium 6

Figure 2: Existing antimalarial drugs..... 12

Figure 3: Life cycle of leishmania parasite..... 16

Figure 4: Drugs available for treatment of leishmania 17

Figure 5: IR spectrum of compound II in nujol 43

Figure 6: ^{1}H NMR spectrum of compound II in $CDCl_3$ 44

Figure 7 : IR spectrum of compound III in nujol..... 47

Figure 8: ^{1}H NMR spectrum of compound III in $CDCl_3$ 48

Figure 9: IR spectrum of compound IIa in nujol 51

Figure 10: ^{1}H NMR spectrum of compound IIa in $CDCl_3$..... 52

Figure 11: IR spectrum of compound IIIa in nujol 55

Figure 12: ^{1}H NMR spectrum of compound IIIa in $CDCl_3$ 56

Figure 13: IR spectrum of compound IIb in nujol 59

Figure 14: ^{1}H NMR spectrum of compound IIb in $CDCl_3$ 60

Figure 15: IR spectrum of compound IIIb in nujol..... 63

Figure 16: ^{1}H NMR spectrum of compound IIIb in $CDCl_3$ 64

Figure 17: IR spectrum of compound IIc in nujol. 66

Figure 18: ^{1}H NMR spectrum of compound IIc in $CDCl_3$..... 67

List of schemes

Scheme 1: Synthesis of pyrazole chalcones under solvent free conditions. 22

Scheme 2: Thermal, solvent-free synthesis of pyrazolyl chalcones. 22

Scheme 3: Synthesis of pyrazolines by reaction of hydrazines and alkyl dihalides 23

Scheme 4: Synthesis of pyrazolines through reaction of dibenzalacetone with hydrazine hydrate and formic acid 23

Scheme 5: Synthesis of pyrazolines by reaction of diazomethane with dimethyl fumarate 24

Scheme 6: Synthesis of pyrazolines through reaction of aryl or alkyl substituted phenylhydrazine with 4- butynol 24

Scheme 7: Synthesis of intermediate α, β unsaturated ketone II 28

Scheme 8: Synthesis of intermediate α, β unsaturated ketone III 29

Scheme 9: Synthesis of acetyl pyrazoline derivative IIa 30

Scheme 10: Synthesis of acetyl pyrazoline derivative IIIa 30

Scheme 11: Synthesis of propyl pyrazoline derivative IIb 31

Scheme 12: Synthesis of propyl pyrazoline derivative IIIb 31

Scheme 13: Synthesis of pyrazoline derivative IIc 32

List of tables

Table 1: Results for physical and elemental microanalyses of the synthesized compounds 40

Table 2: Antimalarial activities for the synthesized compounds at a dose of 48.4 μmol/kg 69

Table 3: Antipromastigote activity (IC_{50}) of the test compounds and reference standards in μg/ml 71

List of acronyms and abbreviations

CL	Cutaneous leishmaniasis
DHF	Dihydrofolate
DHFR	Dihydrofolate reductase
DHODase	Dihydroorotate dehydrogenase
DHPS	Dihydropteroate synthase
Fe(II)PPIX	Ferroheme ferrous-protoporphyrin IX
FV	Parasite food vacuole
GPx	Glutathione peroxidase
HMM	Home-based management of malaria
LLITN	Long-lasting insecticide treated nets
NMCP	National malarial control program
PABA	p-aminobenzoic acid
PC	Phosphatidylcholine
PPM	Parasite plasma membrane
PPPK	Dihydropteridine pyrophosphokinase
SOD	Superoxide dismutase
THF	Tetrahydrofolate
TLC	Thin layer chromatography
TS	Thymidylate synthase
VL	Visceral leishmaniasis

Abstract

Malaria and leishmania are very common parasitic diseases of the developing world and drug resistance has hindered their efficient control. Pyrazole derivatives were synthesized using aldol condensation and subsequent cyclization reactions. The compounds were synthesized in a good yield (71.39%-95.23%). The compounds were purified by recrystallization and their chemical structure was characterized by elemental microanalysis, IR, and ^{1}HNMR spectroscopy. *In vivo* antimalarial and *in vitro* antileishmanial activity was conducted using four day suppression test and Alamar blue reduction method, respectively.

The results for antimalarial activity conducted using *P. berghei* infected mice at a dose level of 48.46μmol/kg/day showed that all the synthesized compounds have lower activity than the standard drug chloroquine phosphate. Compound **IIc**, 1-phenyl-4-(3-(thiophen-2-yl)-4,5-dihydro-1*H*-pyrazol-5-yl)-3-p-tolyl-1*H*-pyrazole, showed relatively the highest % suppression, 63.40%. The result for antileishmanial activity test revealed that all the synthesized compounds except compound **IIb** had better antileishmanial activity than the standard drug miltefosine (IC_{50}= 3.1911 μg/ml). All of the synthesized compounds except compounds **III** and **IIIb** exhibited lower antileishmanial activity compared to the standard drug amphotericin B deoxycholate (IC_{50}=0.0460 μg/ml). Compound **IIIb**, phenyl pyrazoline with propanoyl side chain, 1-(3-phenyl-5-(1-phenyl-3-p-tolyl-1*H*-pyrazol-4-yl)-4,5-dihydropyrazol-1-yl)propan-1-one, was found to be the most active (IC_{50}= 0.0112) and two hundred eighty five and four fold more active than the standards miltefosine and amphotericin B deoxycholate, respectively.

Keywords: pyrazole, *in vivo* antimalarial activity, *in vitro* antileishmanial activity.

1. INTRODUCTION

1.1 Background on malaria

Malaria still remains one of the most important parasitic diseases of the developing world although it is known to humankind since ancient times in different forms. It is caused by Plasmodium parasite. Despite substantial advances in treatment and prevention over the past decade, malaria still threatens the lives of millions in tropical countries. Malaria is a complex disease that varies widely in epidemiology and clinical manifestation in different parts of the world. This variability is the result of factors such as the species of malaria parasites that occur in a given area, their susceptibility to commonly used or available anti-malarial drugs, the distribution of mosquito vectors, climate and other environmental conditions and the behavior and level of acquired immunity of the exposed human populations [1].

In particular, young children, pregnant women, and non-immune visitors to malarious areas are at greatest risk of severe or fatal illness. Many malaria control strategies exist, including long-lasting insecticide treated nets (LLITN) and home-based management of malaria (HMM) which involves presumptively treating febrile children at or near home with antimalarial drugs distributed by trained members of the community. Community distributors provide medications and educate primary caregivers about treatment of malaria, administration of antimalarial drugs, and recognition of severe illness. But none are appropriate and affordable in all contexts. Malaria control and prevention efforts need to be designed for the specific environment in which they will be used and need to take into account the local epidemiology of malaria and the level of available resources and political

will. Parasite resistance to anti-malarial drugs and mosquito resistance to insecticides are major threats to achieving global malaria control [1].

Anti-malarial drug resistance has emerged as one of the greatest challenges facing malaria control today. Drug resistance has been implicated in the spread of malaria to new areas and re-emergence of malaria in areas where the disease had been eradicated. Drug resistance has also played a significant role in the occurrence and severity of epidemics in some parts of the world. Population movement has introduced resistant parasites to areas previously free of drug resistance. The economics of developing new pharmaceuticals for tropical diseases, including malaria, are such that there is a great gap between the public health importance of the disease and the amount of resources invested in developing new cures [2, 3].

This disparity comes at a time when malaria parasites have demonstrated some level of resistance to almost every anti-malarial drug currently available, significantly increasing the cost and complexity of achieving parasitological cure.

1.1.1 Malaria Prevalence and its consequences

Malaria is one of the most prevalent parasitic infections in the world and certainly the most detrimental [4]. In addition to the overwhelming death toll, over 213 million malarial "attacks" lead to more than 800 million days of illness in Africa annually [5].

According to the 2008 WHO report, half of the world's population is at risk of malaria, and an estimated 250 million cases led to nearly 1 million deaths in 2006. According to this report, there were an estimated 247 million malaria cases worldwide, of which 91% were due to *P. falciparum*. The vast majority of cases (86%) were in the African Region, followed by the South- East Asia (9%) and Eastern Mediterranean regions (3%) [6].

The risk of death from malaria is considerably higher in Africa than other parts of the world. There were an estimated 863,000 deaths worldwide in 2008 of which 89% were in the African Region, and 5% in each of the South-East Asia and Eastern Mediterranean regions [1]. It is estimated that the number of cases of malaria to be 225 million and the number of deaths due to malaria to be 781,000 in 2009 [7].

In Ethiopia, malaria is endemic in three quarters of the national territory, with *P. falciparum* predominating over *P. vivax.* In 2006, considerable increase in malaria morbidity had been noted in the south and southwest Ethiopia, possible reasons include climatic changes, drug resistance and migration (e.g. from Sudan) [8]. It is the leading communicable disease in the country. Historically, malaria has forced people to inhabit the agriculturally less productive highlands. This had a negative economic impact, as the country's economy is based on agriculture [9].

An estimated 51 million people (68% of the population) live in areas at risk of malaria. Malaria is still the leading cause of health problem in the country. In 2004, the disease has been reported as the first cause of illness and death accounting for 15.5% of outpatient visits, 20.4% of admissions and 27% of deaths. The magnitude and periodicity of malaria epidemics in the country has also been on the rise in the past few years. Some 5.4 million cases were expected in 2005 [10]. The number of reported malaria deaths in children under 5 years of age dropped from an average of 1866 during 2001-2006 to only 1169 in 2008 which showed a decrease by 37%. The recent decrease in the number of cases and deaths was due to the rapid expansion of control efforts.

Ethiopia had approximately 6% of malaria cases in the African Region in 2006. Malaria is present everywhere except the central highlands. Epidemics are frequent, the last in 2003–2004. Over half of the cases are caused by *P. falciparum*. The national malarial control program (NMCP) distributed 20 million long lasting insecticide treated nets (LLITNs) between 2005 and 2007, targeting 40 million people at risk. The estimated numbers of cases in the country by the year 2006 were 12,405,000 among which 2,073,000 are children under 5 years old. The corresponding number of deaths by the year was 41,000 of which 25,000 were children under 5 years old [6].

Malaria contributes to health problems and deaths on many ways, especially in younger: (1) frequent acute infections, (2) anemia as a result of repeated or chronic malaria infection, (3) malaria in pregnant resulting in low birth weight in the new born and (4) increased susceptibility to other diseases such as respiratory infection, diarrhoea, etc [11].

Malaria is a major obstacle to socioeconomic development in Africa. It accounts for 40% of public health expenditure. Furthermore, the disease not only results in loss of life and productivity because of illness and premature deaths, it also hinders children in their schooling and social development both through absence from school and permanent neurological or other damages associated with severe episodes of the disease [12].

The disease also contributes to poverty. First of all many productive days are lost through sickness or tending to sick relatives. Secondly, the cost of the treatment or barriers to mosquito bites, such as insecticides or mosquito nets is high for the average Africans [12]. Malaria constitutes a major public health problem and impediment to socioeconomic development in Ethiopia [13].

1.1.2 Life cycle of malaria

The malaria parasite exhibits a complex life cycle involving an insect vector (mosquito) and a vertebrate host (human). All four species (*P. vivax, P. ovale, P. falcifarum* and *P. malariae*) exhibit a similar life cycle with only minor variations. The infection is initiated when sporozoites are injected with the saliva of a feeding mosquito. Sporozoites are carried by the circulatory system to the liver and invade hepatocytes. The intracellular parasite undergoes an asexual replication known as exoerythrocytic schizogony within the hepatocyte. Exoerythrocytic schizogony culminates in the production of merozoites which are released into the bloodstream. A proportion of the liver-stage parasites from *P. vivax* and *P. ovale* go through a dormant period instead of immediately undergoing asexual replication. These hypnozoites will reactivate several weeks to months (or years) after the primary infection and are responsible for relapses.

Merozoites invade erythrocytes and undergo a trophic period in which the parasite enlarges. The early trophozoite is often referred to as 'ring form' because of its morphology. Trophozoite enlargement is accompanied by an active metabolism including the ingestion of host cytoplasm and the proteolysis of hemoglobin into amino acids. The end of the trophic period is manifested by multiple rounds of nuclear division without cytokinesis resulting in a schizont. Merozoites bud from the mature schizont, also called a segmenter, and the merozoites are released following rupture of the infected erythrocyte. Invasion of erythrocytes reinitiates another round of the blood-stage replicative cycle [3].

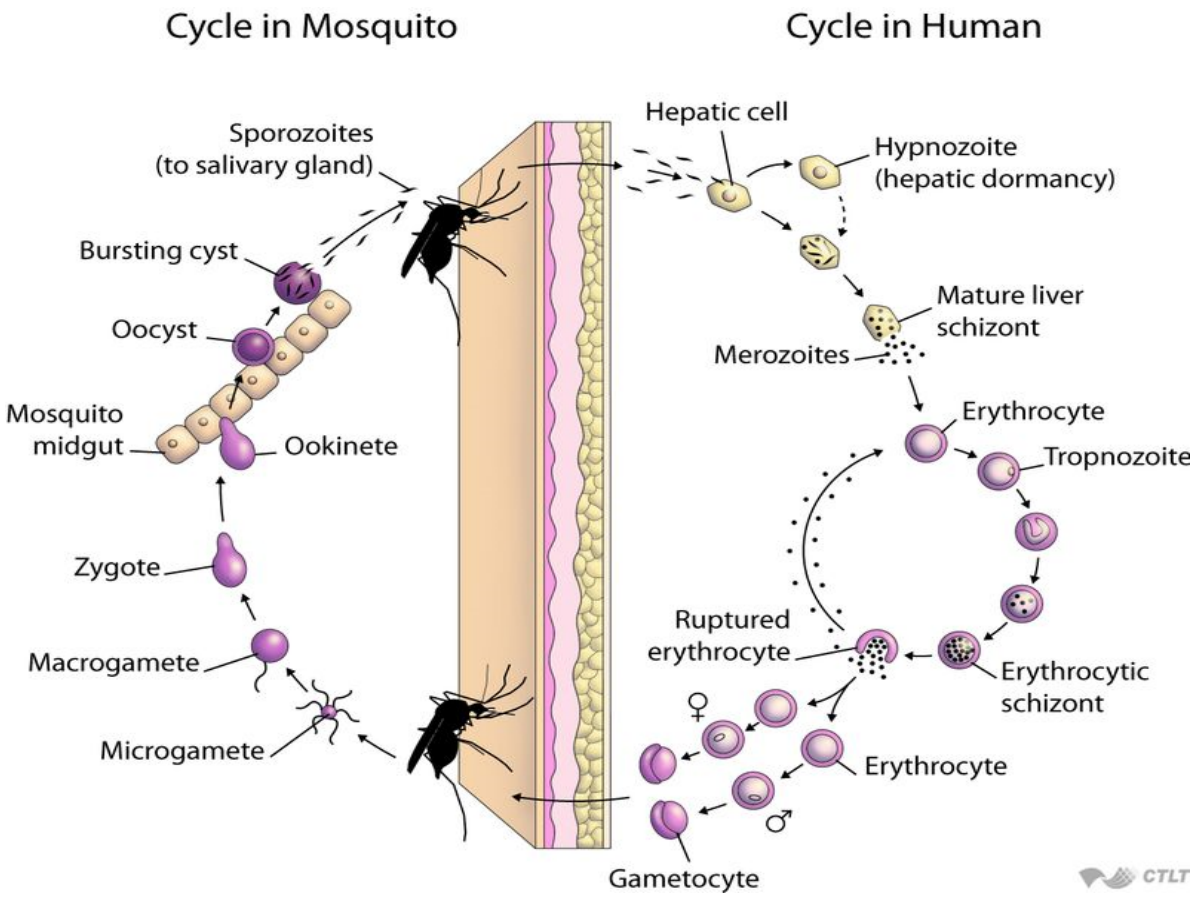

Figure 1: Life cycle of malaria parasite, plasmodium

1.1.3 Drug targets for antimalarial treatment

The control of malaria largely depends on drug therapies, and, to a lesser extent, prophylaxis. Most of the antimalarial drugs available currently have been in use for decades, but their use is now severely limited by the emergence and spread of drug resistance, primarily against *P. falciparum*, the malaria parasite that causes severe forms of disease and most of the disease burden. We need to know more about sites of parasite vulnerability and the basic mechanisms through which drugs act and resistance is generated in order not only to generate new drugs with novel mechanisms of action, but also to make better use of the drugs that we have [14].

1.1.3.1 Nucleic acid inhibitors

1.1.3.1.1 Folate antagonists

Some of the most widely used antimalarial drugs belong to the folate antagonist class. Inhibition of enzymes of the folate pathway results in decreased pyrimidine synthesis, hence, reduced DNA, serine, and methionine formation. Activity is exerted at all growing stages of the asexual erythrocytic cycle and on young gametocytes. Traditionally, antifolates are classified into two classes: [14]

A- Type-1 antifolates (sulfonamides and sulfones) mimic p-aminobenzoic acid (PABA). They prevent the formation of dihydropteroate from hydroxymethyldihydropterin (strictly speaking, the pyrophosphate derivative) catalyzed by dihydropteroate synthase (DHPS) by competing for the active site of DHPS (a bifunctional enzyme in plasmodia coupled with 2-amino-4-hydroxy-6-hydroxymethyl-dihydropteridine pyrophosphokinase [PPPK]) [14].

B- Type-2 antifolates (pyrimethamine, biguanides and triazine metabolites, quinazolines) inhibit dihydrofolate reductase (DHFR, also a bifunctional enzyme in plasmodia coupled with thymidylate synthase [TS]), thus preventing the NADPH-dependent reduction of H_2folate (DHF) to H_4folate (THF) by DHFR. THF is a necessary cofactor for the biosynthesis of thymidylate, purine nucleotides, and certain amino acids. DHFR inhibitors mimic the pteridine ring of the natural substrate DHF, and compete with it for the active site of the enzyme. Pyrimethamine and cycloguanil have a phenyl pyrimidine and a dihydrodiazine group, respectively, that fits the hydrophobic active site pocket of DHFR and that forms H-bonds with the carboxyl oxygens of Asp54 (in helix B), as DHF does [14].

1.1.3.1.2 DHODase blockers

Atovaquone {2-[trans-4-(4′ -chlorophenyl)cyclohexyl]-3- hydroxy-1,4-naphthoquinone}, a hydroxynaphthoquinone, is used for both the treatment and prevention of malaria in a fixed

combination with proguanil. Whilst known to act primarily on mitochondrial functions, its mode of action and synergy with proguanil are not completely understood. This matter is further complicated by the diverse functions of mitochondria in various organisms and by technical difficulties with experiments. It is generally agreed that atovaquone acts on the mitochondrial electron transfer chain, although more recently, its activity and synergy with proguanil has been ascribed to its interference with mitochondrial membrane potential. The two are intimately linked; as the mitochondrial electron transport chain serves to generate this membrane potential. One proposed site for atovaquone's activity is dihydroorotate dehydrogenase (DHODase), a critical enzyme in electron transport. Inhibition of DHODase blocks pyrimidine synthesis. DHODase catalyses the conversion of dihydroorotate to orotate. It bridges pyrimidine *de novo* synthesis and the mitochondrial electron transport system, and is also the major source of electrons for the mitochondrial electron transport chain [14].

1.1.3.2 Blood schizontocides

Blood schizontocides are drugs that act on intra-erythrocytic (asexual and partly also sexual) forms of parasites. Their primary target is believed to be the parasite food vacuole (FV). They include quinoline-containing drugs and the artemisinin-type compounds [14].

1.1.3.2.1 Haem disposal

The quinoline-containing drug class includes some of the most common antimalarial drugs: type-1 drugs (the 4-aminoquinolines chloroquine and Mannich-base amodiaquine, pyronaridine) and type-2 drugs (the aryl-amino alcohols quinine and quinidine, mefloquine, halofantrine). The two groups differ in that type-1 drugs are weak bases, diprotonated and hydrophilic at neutral pH, whereas type-2 drugs are weaker bases and lipid soluble at neutral pH. In addition, the two groups appear to interact differently with their putative target and show an inverse relationship with respect to parasite sensitivities [14].

The commonly accepted hypothesis is that quinoline containing drugs act primarily on haem disposal, a process whereby intra-erythrocytic-stage malaria parasites detoxify haem in the FV. There are conflicting data as to whether such a mechanism would explain the mode of action of both chloroquine and the quinoline/phenantrene methanols. However, recent experiments using proteinase inhibitors and quinoline-containing drugs substantiate the view that interaction with haem is central to the activity of this class of compounds [14].

1.1.3.2.2 Free radical formation

The artemisinin-type compounds in current use are either the natural extract artemisinin itself or the semi-synthetic derivatives (dihydroartemisinin, artesunate, artemether, arteether). They achieve higher reduction rates of parasitaemia per cycle than any other drug known to date, and are being used for the treatment of uncomplicated and severe forms of malaria [14].

All members of this drug group have activity throughout the phases of the asexual intra-erythrocytic schizogonicycle, and also act on young gametocytes. The mechanism of action is incompletely understood, but the prevailing hypothesis is that reductive cleavage of the intact peroxide by ferroheme ferrous-protoporphyrin IX (Fe(II)PPIX) generates C-centered radicals, which, in turn, would alkylate biomolecules, leading to the death of the parasite [14].

1.1.4 Novel molecular targets

1.1.4.1 Parasite membrane biosynthesis

Intraerythrocytic parasites possess different membranes such as the food vacuolar membrane, the parasite plasma membrane (PPM) and the parasitophorous vacuole membrane. The amount of lipid in infected erythrocytes is therefore significantly higher than that of normal erythrocytes. Growing and dividing malaria parasites require large amounts of phospholipids, which are synthesized from plasma fatty acids. Phosphatidylcholine (PC) is the major

parasite phospholipid. Most of the PC (70–80%) is synthesized by de novo synthesis from choline [15].

1.1.4.2 Parasite transporters

There is a profound increase in the permeability of the host membrane to a wide range of solutes in malaria-infected erythrocytes. Molecular traffic across the host erythrocyte membrane undergoes dramatic changes with respect to intensity and the nature of permeating solutes. The induced permeability pathways are known as new permeability pathways (NPPs), which are polyspecific, anion selective and confer increased permeability to a wide range of charged and low-molecular-weight solutes [15]. These NPPs are thought to provide the major entry of some essential nutrients (pantothenate) required by the parasites. They also mediate the efflux of various metabolic waste substances such as lactic acid from the infected cell. The properties of the parasite induced transport systems are significantly different from those in normal human cells. Therefore, these transport systems could potentially be exploited as targets for antimalarial chemotherapy. This could be achieved by designing cytotoxic drugs that selectively enter the parasite through these induced transporter routes [15].

1.1.4.3 Parasite proteases

Plasmodia are blood-eating parasites. Proteases have an important role in parasite survival by hydrolyzing a significant proportion of the host erythrocyte proteins. Approximately 80% of the host cell haemoglobin is broken down into individual amino acids, some of which are used for parasite protein synthesis. Several *Plasmodium* proteases that appear to be responsible for vital cleavage of host proteins have been characterized [15].

1.1.4.4 The redox system

Oxidative stress is an important mechanism for destruction of malaria and other intracellular parasites. In intraerythrocytic-stage malaria, parasites encounter reactive oxygen species produced either by themselves or by the erythrocyte or host immune cells. To prevent oxidative stress, the parasite has its own battery of defense tactics and produces its own antioxidant enzymes. The malaria parasite contains three antioxidant enzymes: superoxide dismutase (SOD), glutathione peroxidase (GPx) and catalase. The parasite's antioxidant defense could therefore be a potential target for antimalarial chemotherapeutics [15].

1.1.5 Drugs currently used against malaria

For decades, malaria chemotherapy has relied on a limited number of drugs. However, the acquisition and spread of drug resistance has led to an increase in morbidity and mortality rates in many malaria-endemic regions. This increasing burden caused by drug-resistant parasites has stimulated investigators to seek out novel antimalarial drugs [2].

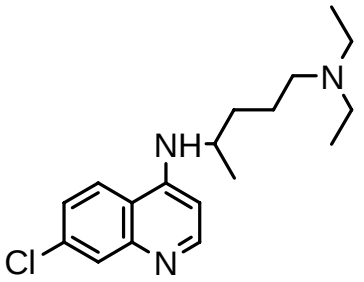

Chloroquine

1

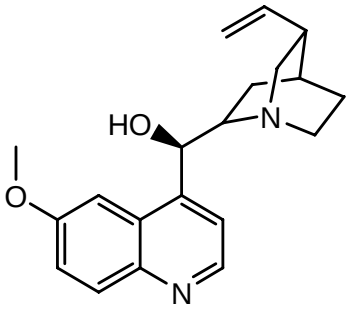

Quinine

2

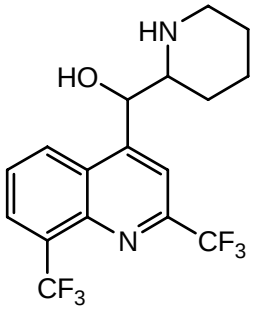

Mefloquine

3

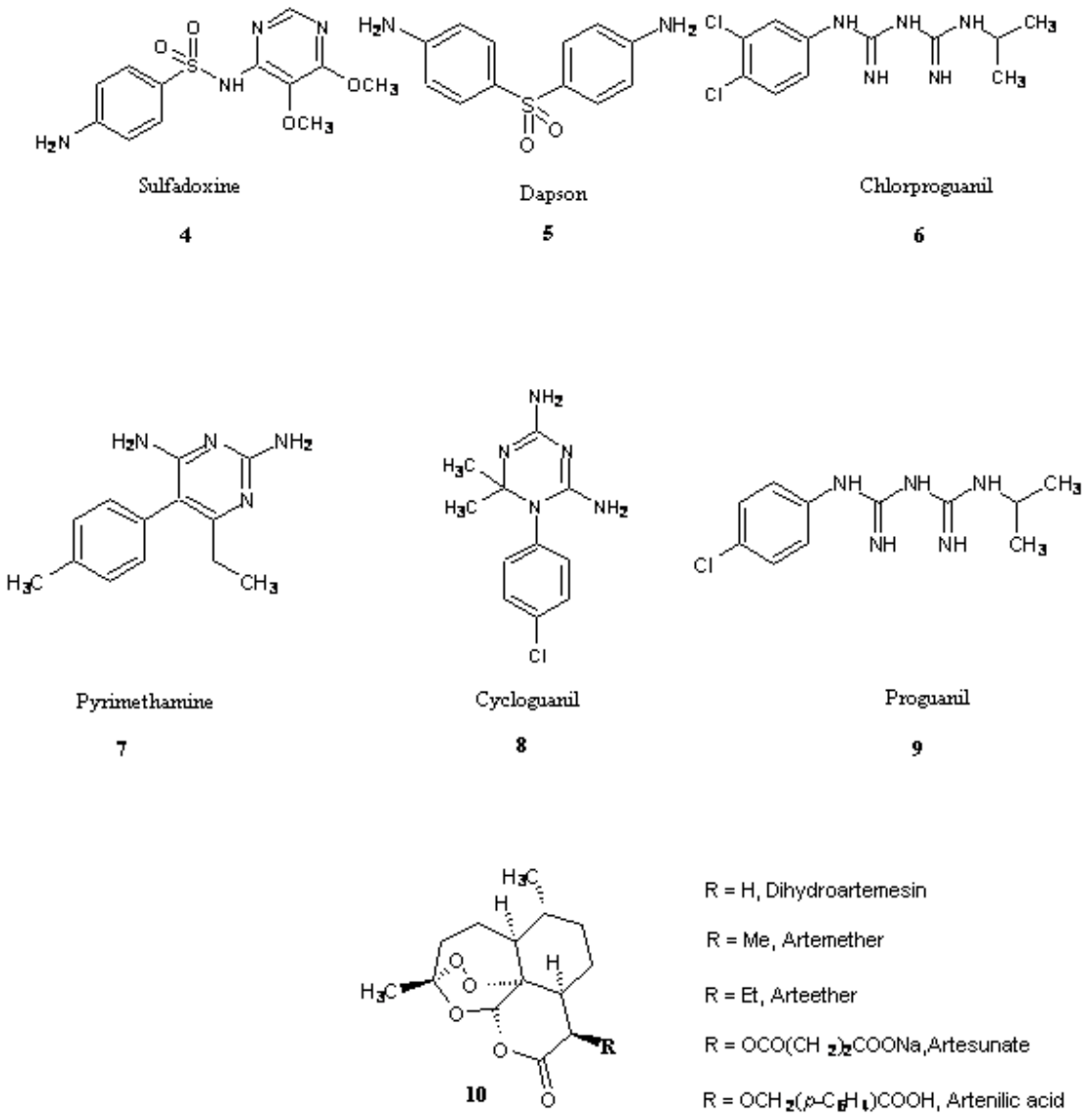

Figure 2: Existing antimalarial drugs

1.1.6 Antimalarial drug resistance

Several medicines ranging from chloroquine to currently used medicines, such as sulfadoxine–pyrimethamine, mefloquine have sequentially fallen to resistance, in particular in the case of *P. falciparum* malaria, and have thus become ineffective for treatment in many parts of the world [16].

Moreover, according to research report in 2008, the current and widely used drug, artemisinin is losing its potency in Cambodia and increased efforts are required to prevent drug-resistant malaria from spreading across the globe [16].

1.2 Background on leishmaniasis

Leishmaniasis is an infection caused by various species of Leishmania protozoa, which are usually transmitted by the bite of various species of phlebotomine sandflies [17]. There are four main forms of leishmaniasis.

- *Localized cutaneous leishmaniasis* is characterized by an itchy lesion on an arm or leg or the face, and possibly swollen lymph nodes in the same area. Over a period of months, the sore will develop a red raised edge and a central crater (ulcer). It may heal on its own, or invade and destroy surrounding tissue [18].
- *Diffuse cutaneous leishmaniasis* is similar, except the lesions spread all over the body and resemble leprosy [18].
- *Mucocutaneous leishmaniasis* begins with the type of sores that indicate localized cutaneous leishmaniasis, but years after those lesions heal, new ones appear in the mouth and nose, or occasionally near the genitals. The new sores are painful, erode underlying tissue, and are vulnerable to bacterial infection. Other symptoms include fever, weight loss, and anemia [18].
- *Visceral leishmaniasis* is the most serious form of the disease. Lesions appear on the skin and the skin takes on a grayish color. Protozoa travel through the bloodstream to the liver, spleen, lymph nodes and bone marrow. Weakness, diarrhea, and weight loss are common. The disease is usually caused by *L. donovani* or *L. infantum*, protozoan parasites transmitted to human and animal hosts by the bite of phlebotomine sand flies [18].

1.2.1 Epidemiology of leishmaniasis

Human leishmaniasis is found in five continents and is endemic in the tropical and sub-tropical regions of 16 'developed' and 72 'developing' countries, including 13 of the world's least developed countries [19].

Globally, there are believed to be approximately 12 million cases, with 1.5 million to 2 million new cases of cutaneous leishmaniasis (CL) and 500,000 new cases of visceral leishmaniasis (VL) each year. Sixty-two countries have endemic VL, and the geographical distribution of this disease is expanding in several areas of the world [19]. Leishmaniasis is reported endemic in 88 countries, of which 82% are low-income countries [20].

East Africa is one of the world's main endemic areas for VL, which over the last 20 years has seen a dramatic increase in the number of VL cases, due to a complexity of factors [21]. Several studies have convincingly shown that malnutrition, HIV and genetic susceptibility are individual risk factors for VL [22, 23].

Culturing of Leishmania promastigotes from scrapings or biopsies has been shown to be more sensitive for diagnosis of *L. aethiopica*, the main causative agent of CL in Ethiopia [24]. CL in Ethiopia is known to be caused mainly by two species, *L. aethiopica* and *L. major*. An extensive molecular study in this particular endemic setting suggests that the majority of cases are caused by *L. aethiopica* [25].

1.2.2 Life cycle of leishmania parasite

The sandfly vector becomes infected when feeding on the blood of an infected individual or an animal reservoir host. The leishmania parasites live in the macrophages as round, non-motile amastigotes (3-7 micrometers in diameter). The macrophages are ingested by the fly during the blood- meal and the amastigotes are released into the stomach of insect. Almost immediately the amastigotes transform into the motile, elongated (10-20 micrometers), flagellate promastigote form [25]. The promastigotes then migrate to the alimentary tract of the fly, where they live extracellularly and multiply by binary fission. Four to five days after feeding, the promastigotes move forward to the oesophagus and the salivary glands of the insect. When the sandlfy next feeds on a mammalian host, its' proboscis pierces the skin and saliva containing anti-coagulant is injected into the wound to prevent the blood from clotting, the leishmania promastigotes are transferred to the host along with the saliva. Once in the host the promastigotes are taken up by the macrophages where they rapidly revert to the amastigote form. The leishmania are able to resist the microbiocidal action of the acid hydrolases released from the lysozymes and so survive and multiply inside the macrophages, eventually leading to the lysis of the macrophages. The released amastigotes are taken up by additional macrophages and so the cycle continues. Ultimately all the organs containing macrophages and phagocytes are infected, especially the spleen, liver and bone marrow [25].

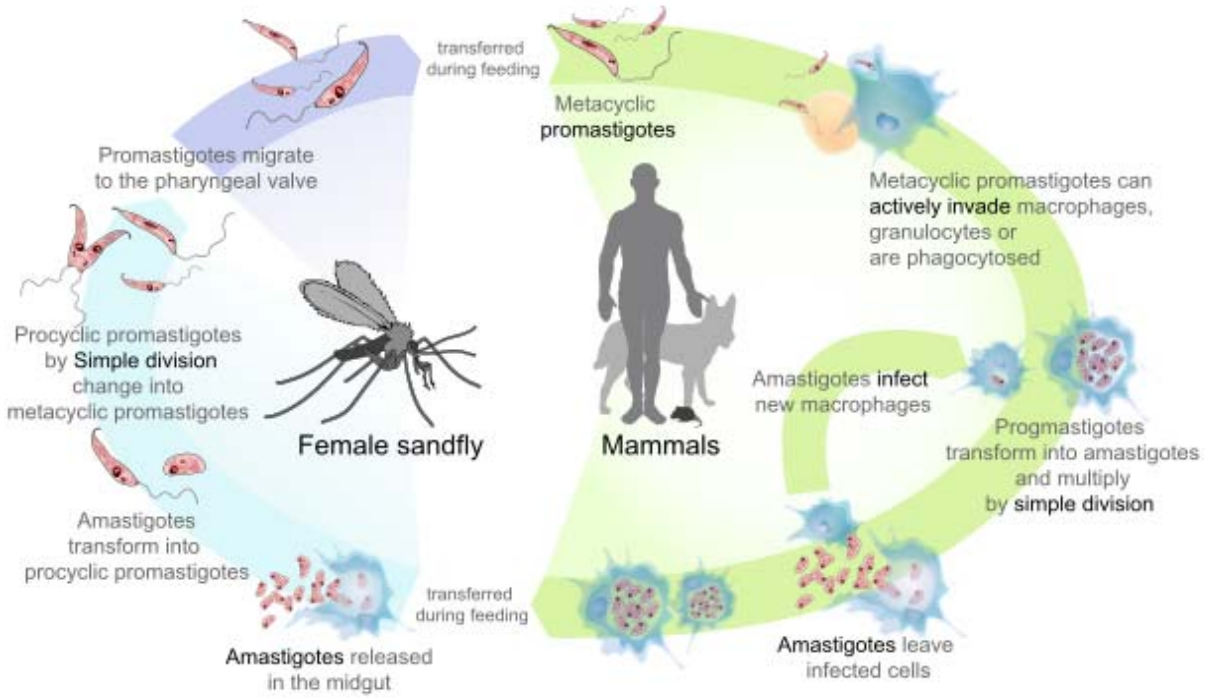

Figure 3: Life cycle of leishmania parasite

1.2.3 Drugs available for treatment of leishmaniasis

Chemotherapeutic treatment of leishmaniasis usually relies on the use of pentavalent antimonials such as sodium stibogluconate (pentostan) (**11**) and meglumine antimoniate (glucantime) (**12**) that induce toxic side effects together with drug resistance [26].

Unfortunately, in many parts of the world, the parasite has become resistant to antimony.

Amphotericin (AmBisome) (**13**) is now the treatment of choice [27]. Its failure in some cases to treat visceral leishmaniasis (*L. donovani*) has been reported in Sudan [28], but this may be related to host factors such as co-infection with HIV or tuberculosis rather than parasite resistance. Miltefosine (Impavido) (**14**) is a new drug for visceral and cutaneous leishmaniasis. Paromomycin (**15**) is said to be an inexpensive and effective treatment for leishmaniasis.

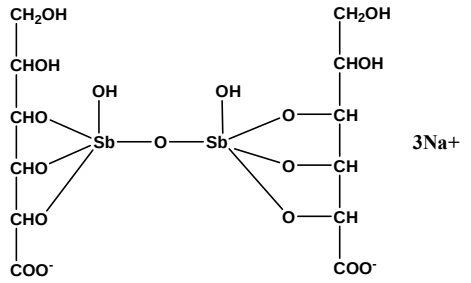

11

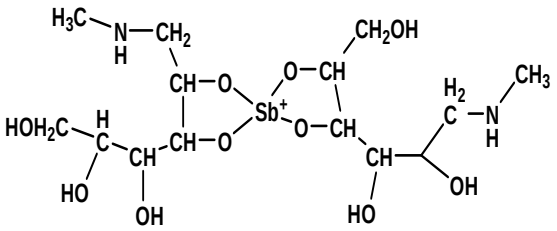

12

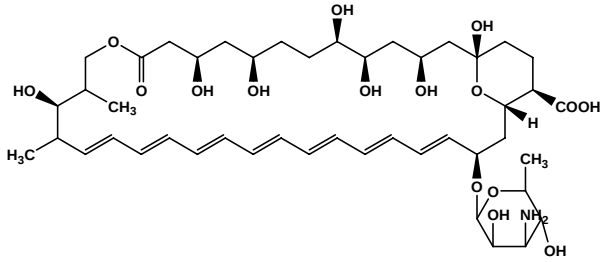

13

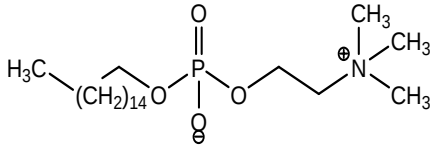

14

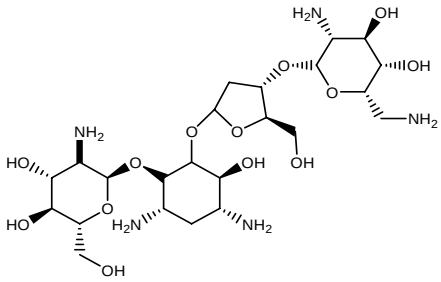

15

Figure 4: Drugs available for treatment of leishmania

1.3 Pyrazole derivatives as biologically active compounds

Different pyrazole derivatives were found to possess various important biological activities such as; antibacterial (**16 & 17**) [29,30], antiinflammatory (**18 & 19**) [31,32], antioxidant (**20**) [33], ACE inhibitory (**21**) [34], anti-cancer (**22**) [35], MAO-B inhibitory (**23**) [36], antidepressant (**24**) [37], antiviral (**25**) [38], antimycobacterial (**26 & 27**) [39,40], antileishmanial (**28 & 29**) [41,42], and antimalarial (**30 & 31**) [43,44] activities. These promising findings and continuation of the efforts to find a new class of antimalarial and antileishmanial agents initiated research on such hetrocyclic compounds.

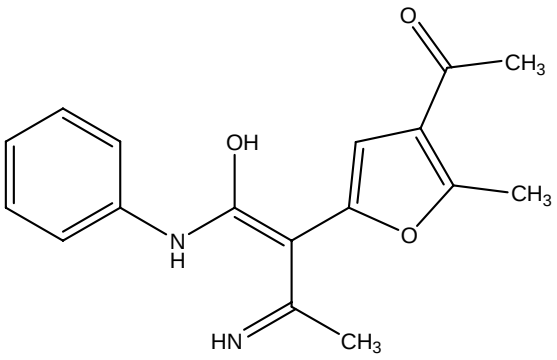

16

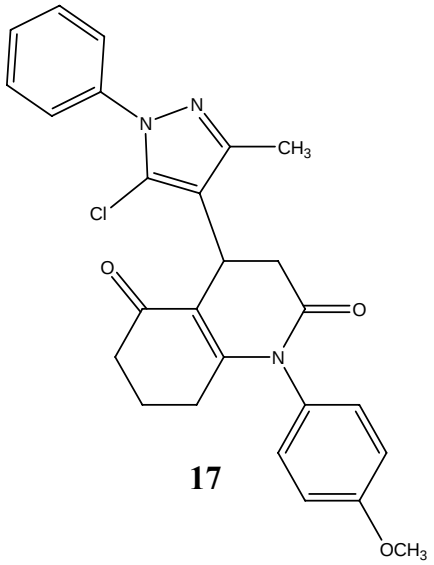

17

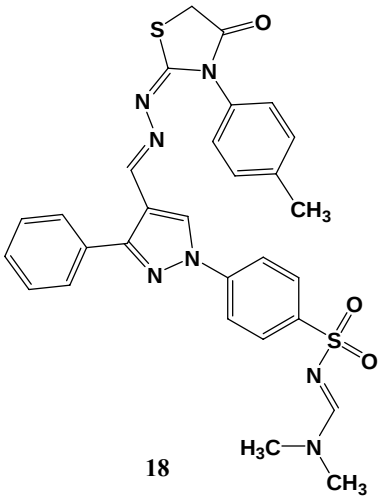

18

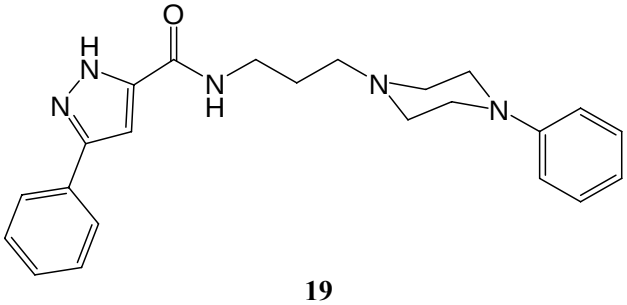

19

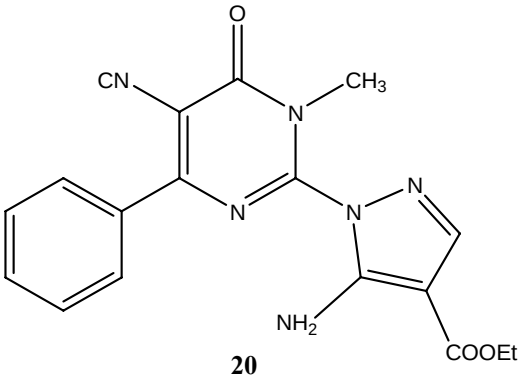

20

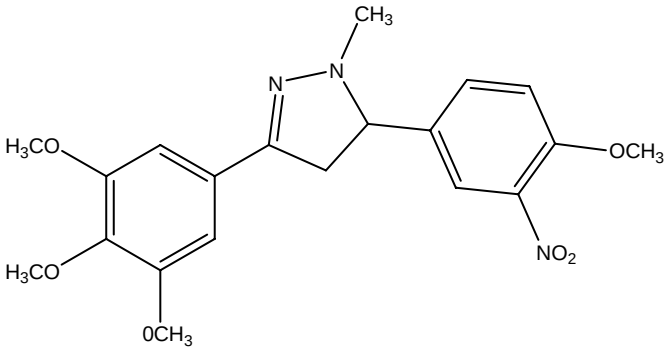

21

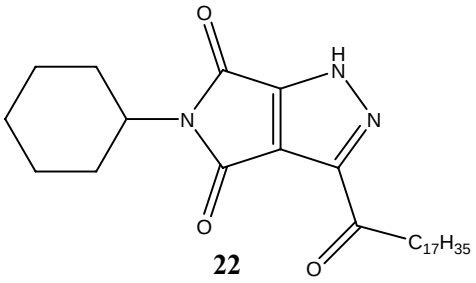

22

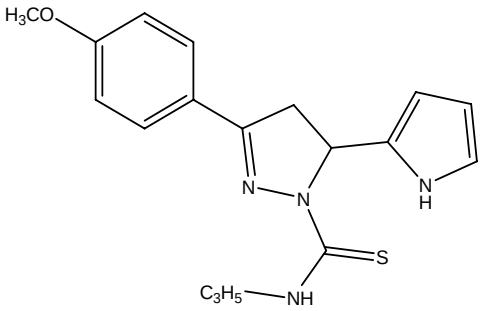

23

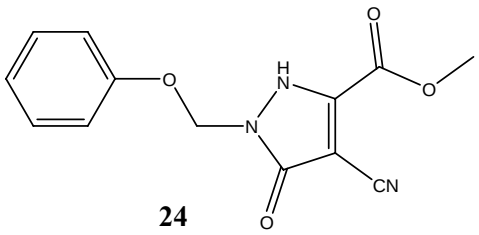

24

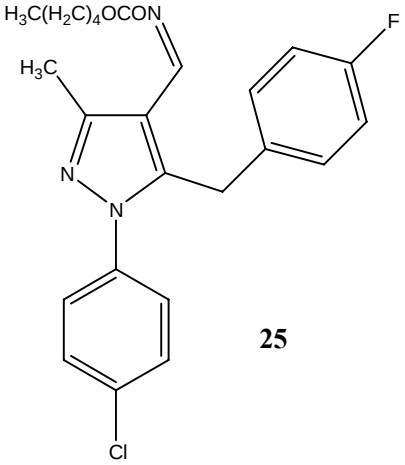

25

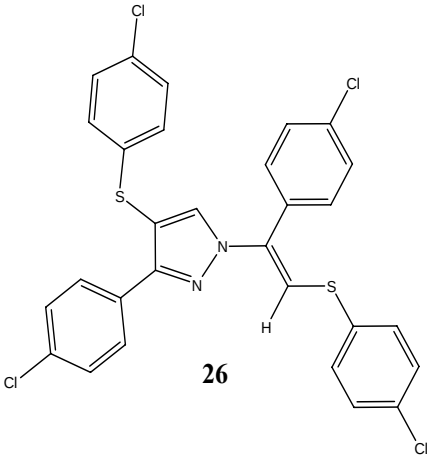

26

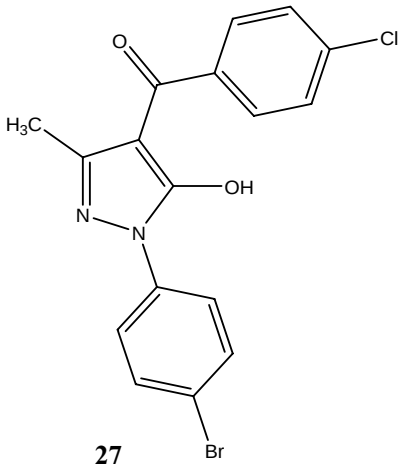

27

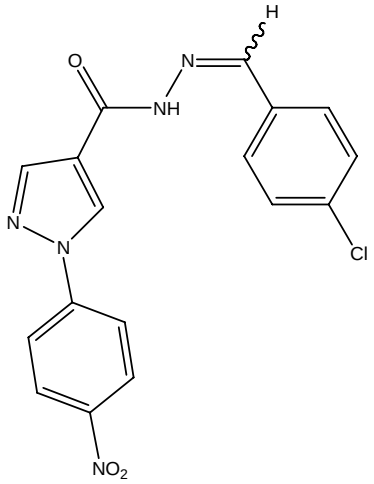

28

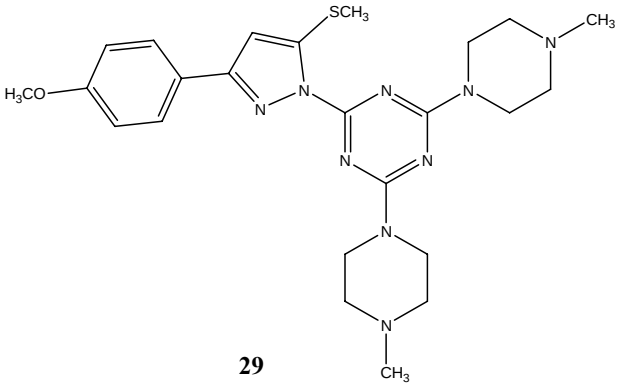

29

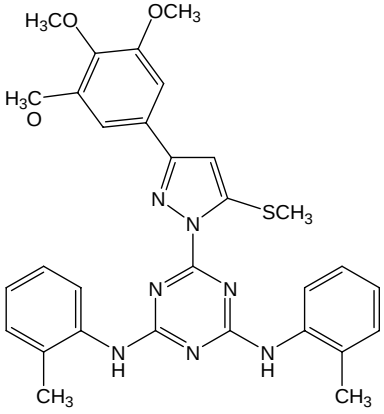

30

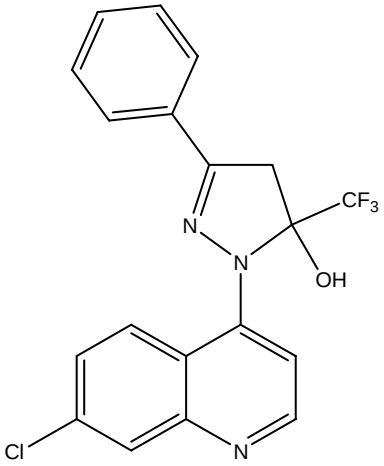

31

Pyrazoline derivatives were reported to possess significant antileishmanial and antimalarial activity (**32**) [45]. Based on these promising findings, as a continuation to our ongoing program to find effective, safe and cheap antimalarial and antileishmanial agent, this project has been designed to synthesize and investigate pyrazoline derivatives containing phenyl or thiophenyl moiety in our research laboratory.

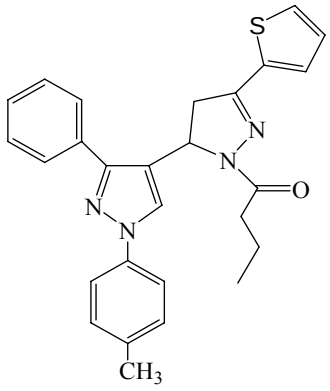

32

1.4 Reported methods for synthesis of pyrazole chalcones

Chalcones are an important class of compounds extensively distributed in nature and considered as the precursors for flavonoid synthesis in plants. Chemically they consist of an open chain in which the two aromatic rings are connected by a three-carbon α,β-unsaturated carbonyl system. In recent years, chemistry of chalcones has fascinated interest as these compounds have been found to exhibit several biological activities, such as cytotoxic, antimalarial, antileishmanial, antiinflammatory and anti-HIV activities [46].

There are different methods for the synthesis of pyrazole chalcones that are reported in literatures. Some of them are the following

1.4.1 Synthesis of pyrazole chalcones under solvent free conditions at room temperature

An easy, safe, solvent free and effective method for the synthesis of pyrazole-substituted chalcones has been achieved by grinding pyrazole aldehydes and acetophenones in the presence of activated barium hydroxide in high yield within short span of time [46].

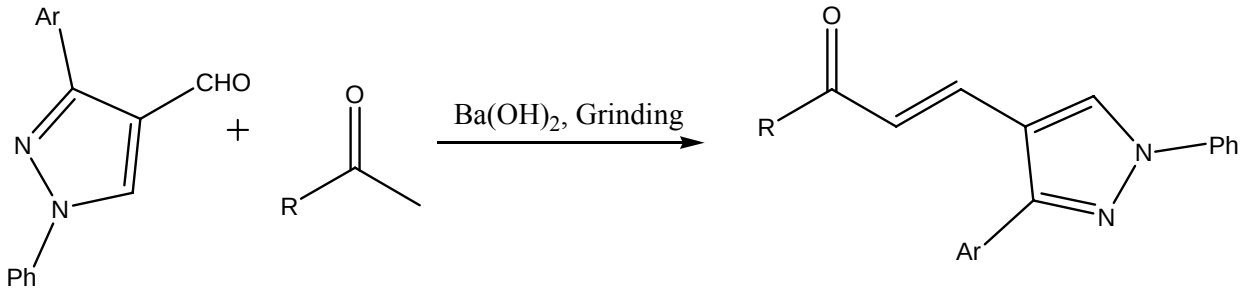

Scheme 1: Synthesis of pyrazole chalcones under solvent free conditions.

1.4.2 Thermal solvent-free synthesis

A novel approach of thermal solvent-free synthesis of pyrazolyl chalcones was adopted for the synthesis of a series of new pyrazolyl chalcones by the reaction of 5-chloro-3-methyl-1-phenylpyrazole-4-carboxaldehyde with different 5-acetylbarbituric acid derivatives under thermal solvent-free condition [47].

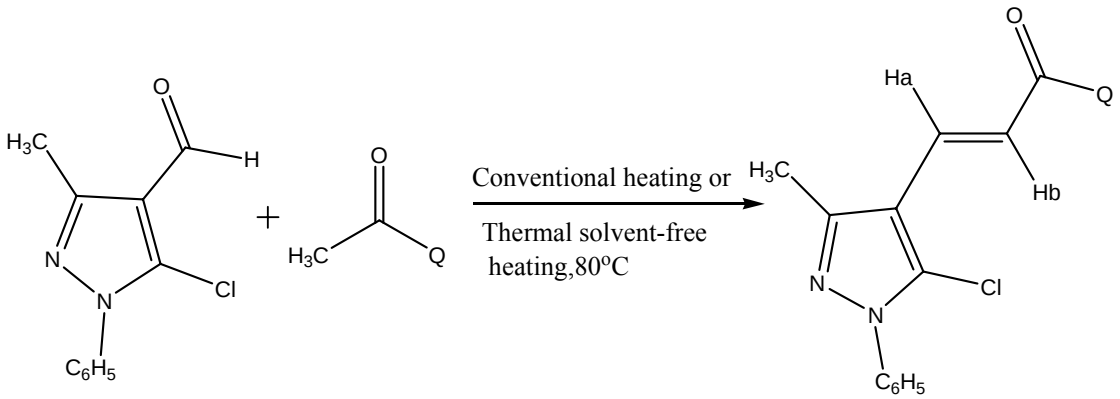

Scheme 2: Thermal, solvent-free synthesis of pyrazolyl chalcones.

1.5 Reported methods for synthesis of pyrazolines

There are various methods for the synthesis of pyrazoline derivatives reported in literature**.** Some of them are described below.

Pyrazolines can be synthesized by reaction of alkyl dihalides and hydrazines under microwave irradiation *via* a simple and efficient cyclocondensation in an alkaline aqueous medium [48].

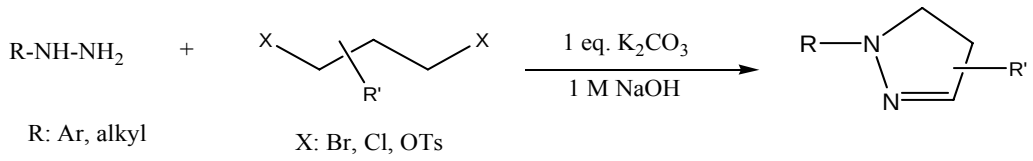

Scheme 3: Synthesis of pyrazolines by reaction of hydrazines and alkyl dihalides

The other synthetic method to produce pyrazolines is through the reaction of α, β unsaturated ketones with diazomethanes or hydrazine derivatives. It was reported that the reaction of dibenzalacetone and hydrazine hydrate with formic acid by heating under reflux for 24 hr under constant stirring gave 5- phenyl-3-(2-phenylvinyl]-4,5-dihydro- 1*H*-pyrazole-1-carbaldehyde [49].

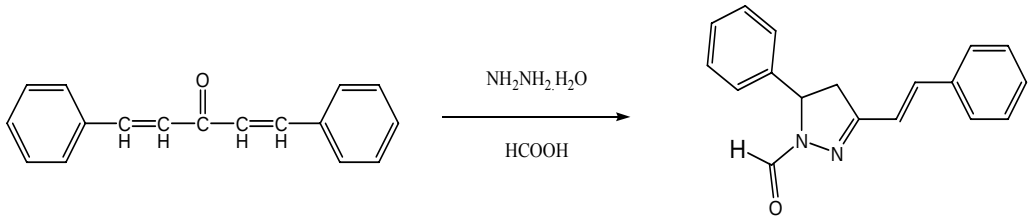

Scheme 4: Synthesis of pyrazolines through reaction of dibenzalacetone with hydrazine hydrate and formic acid

It was reported that the diazomethane leads to the formation of pyrazoline type compound on reaction with dimethyl fumarate. The primary product of such cycloaddition is 1- pyrazoline but it spontaneously isomerizes into the more thermodynamically stable compound, 2-pyrazoline by 1, 3- hydride shift [50].

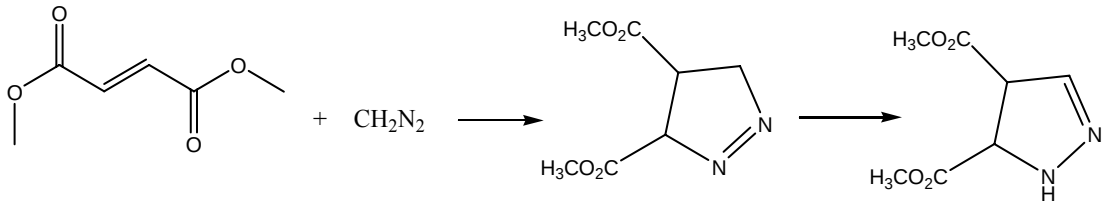

Scheme 5: Synthesis of pyrazolines by reaction of diazomethane with dimethyl fumarate

When arylhydrazines regioselectively react with 4-butynol in the presence of a catalytic amount of zinc triflate, aryl-substituted pyrazolines are obtained. [51].

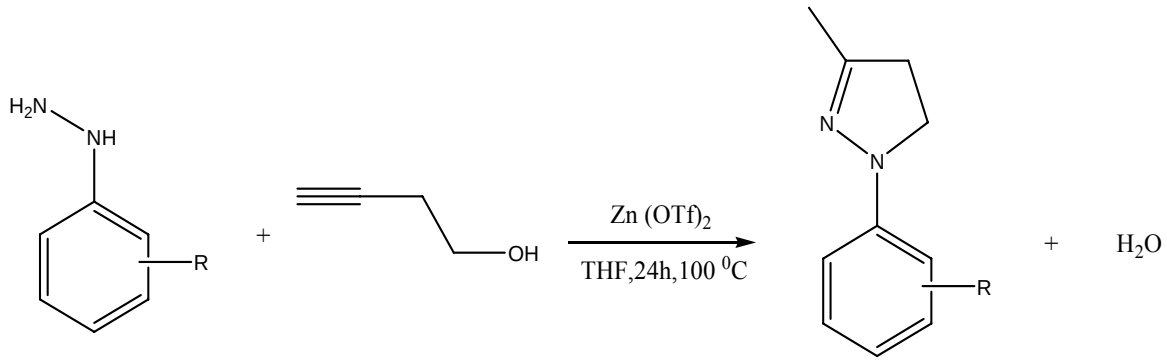

Scheme 6: Synthesis of pyrazolines through reaction of aryl or alkyl substituted phenylhydrazine with 4- butynol

2 OBJECTIVES

2.1 General objective

- To synthesize some pyrazole derivatives and evaluate their antimalarial and antileishmanial activities.

2.2 Specific objectives

- To synthesize some pyrazole derivatives by applying aldol condensation and Michael addition reaction.
- To elucidate the chemical structures of the synthesized compounds using some physical and spectroscopic techniques like ^{1}H NMR and IR spectroscopy.
- To evaluate *in vivo a*ntimalarial activities of the synthesized compounds on *P. berghei* compared to the standard reference drug Chloroquine.
- To evaluate *in vitro* antileishmanial activity of the synthesized compounds relative to the standard drugs.
- To try to find structure activity relationships of the synthesized compounds for both anti-malarial and antileishmanial activities.

3 EXPERIMENTAL

3.1 Materials Used

3.1.1 Chemicals and Reagents

Acetophenone, 2-acetylthiophene and hydrazine hydrate (Sigma Aldrich), ethanol, glacial acetic acid, propanoic acid, hydrochloric acid, KOH, absolute methanol, acetonitrile, chloroform, ethyl acetate, benzene, Tween 80, normal saline, sodium citrate, distilled H_2O, dimethyl sulfoxide (BDH, England), Giemsa, alamar blue, RPMI 1640 have been used

throughout the experiments. 1-phenyl-3-p-tolyl-1H-pyrazole-4-carbaldehyde was donated by Drug Discovery Centre, Department of pharmaceutical chemistry, Faculty of Pharmacy, Alexandria University, Egypt.

3.1.2 Instruments and apparatus

Silica gel thin layer chromatography (TLC) plates (Merck, Germany) of 0.25 mm thickness were used for chromatographic purposes and the spots were visualized with the aid of UV light and iodine vapor. ^{1}H NMR spectral data were collected using a Bruker Avance DMX400 FT NMR spectrometer at the Department of Chemistry, Faculty of Science, Addis Ababa University, Ethiopia. Splitting patterns of ^{1}H NMR spectra are designated as follows: s, singlet; d, doublet, dd, doublet of doublet; t, triplet and m, multiplet. Chemical shift values were given in parts per million and coupling constants (J) in Hertz. IR spectra were recorded on a Shimadzu 8400SP Spectrophotometer in the range of 4000- 500 cm^{-1} at Ethiopian pharmaceutical factory (EPHARM). Melting points were determined on electro thermal IA9100 hot storage melting point apparatus and in an open melting tube on an electro thermal melting point apparatus, at Ethiopian health and food nutrition research institute (EHNRI). Elemental analytical data were obtained using Perkin Elmer 2400 elemental analyzer at Microanalytical unit, Faculty of science, Cairo University, Egypt. Malaria parasites were counted using BIO-PLUS microscope at the Department of biology, Addis Ababa University, Ethiopia. In addition micropipettes (pipetman ultra), oven (Gallenkamp), haemocytometer (for counting leishmania parasites), eppendroff tube, normal and inverted microscope (Motic and Olymus), heating mantle, autoclave (Pristage), thermoshake (Gerhardt), Vortex (model- whirl VIB2), pipette tips (Oxford), slides, aluminum foil, suction

filter, class II biosafety cabinet (Labconco) have been used throughout the experiment for anti-leishmania activity test.

3.1.3 Experimental animals and parasite strain

Swiss albino mice of both sex, weighing 24-38 g and of age 4-6 weeks obtained from Ethiopian Health and Nutrition Institute were used in testing the antimalarial activity. The animals were acclimatized for a period of 7 days at room temperature (23-25 $^{\circ}$C) and relative humidity of 60-65% before starting the assay. The animals were housed in standard cages and maintained on standard pellated diet and water. The rodent malaria parasite, *P. berghei* ANKA strain was obtained from the biomedical laboratory at the Department of biology, Faculty of Science, Addis Ababa University, Ethiopia. *L. donovani,* a leishmanial parasite that causes visceral leishmaniasis in Africa was used for the antileishmanial testing.

3.1.4 Standard Drugs

Chloroquine phosphate (EPHARM) was used as a reference drug in determination of the antimalarial activity of the synthesized compounds. Amphotericin B deoxycholate (Fungizone®, E R Squibb, UK) and miltifosine/ hexadecylphosphocholine (A G Scientific, San Diego, CA, USA) were used as standard drugs in the determination of the antileishmanial activity of the synthesized compounds.

3.2 Methods

3.2.1 Synthesis of target compounds

The intermediate α, β unsaturated ketones, (**II** and **III)** were synthesized by aldol condensation of 1-phenyl-3-p-tolyl-1H-pyrazole-4-carbaldehyde **I** with 2-acetylthiophene and acetophenone respectively in alcoholic KOH. The target thienyl and phenyl pyrazolines were synthesized by cyclization of the intermediate α, β unsaturated ketones (**II** and **III)** with hydrazine hydrate in ethanol or the appropriate aliphatic acid.

(E)-3-(1-phenyl-3-p-tolyl-1*H*-pyrazol-4-yl)-1-(thiophen-2-yl)-prop-2-en-1-one (II)

One of the intermediate compounds, which is an *α, β* unsaturated ketone **II** was synthesized by condensation of 1-phenyl-3-p-tolyl-1H-pyrazole-4-carbaldehyde **I** (2 g, 7.63 mmol) with 2-acetylthiophene (0.96 g, 7.63 mmol) in 20% ethanolic solution of KOH (20 ml). The yellow precipitate formed was filtered, washed with ethanol, dried and then recrystallized from chloroform/ethanol mixture (4:1).

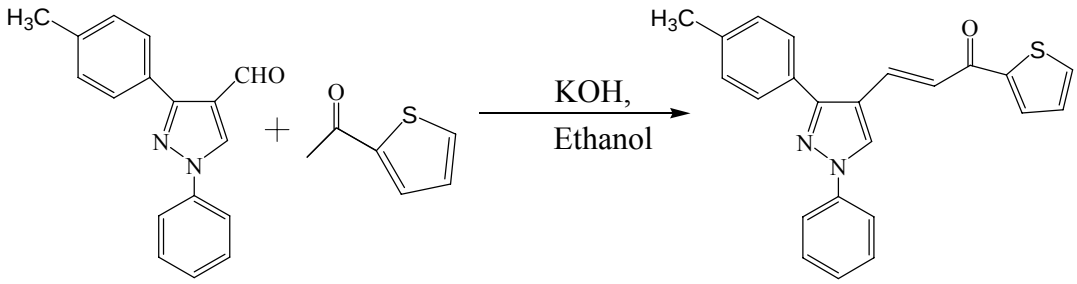

Scheme 7: synthesis of intermediate α, β unsaturated ketone **II**

(E)-1-phenyl-3-(1-phenyl-3-p-tolyl-1*H*-pyrazol-4-yl)-prop-2-en-1-one (III)

The other intermediate compound, which is also an α, β unsaturated ketone **III** was synthesized by condensation of 1-phenyl-3-p-tolyl-1H-pyrazole-4-carbaldehyde **I** (1 g, 3.81 mmol) with acetophenone (0.457 g, 3.81 mmol) in 20% ethanolic solution of KOH (20 ml). The yellow precipitate was filtered, washed with ethanol, dried and then recrystalized from chloroform/ethanol mixture (4:1).

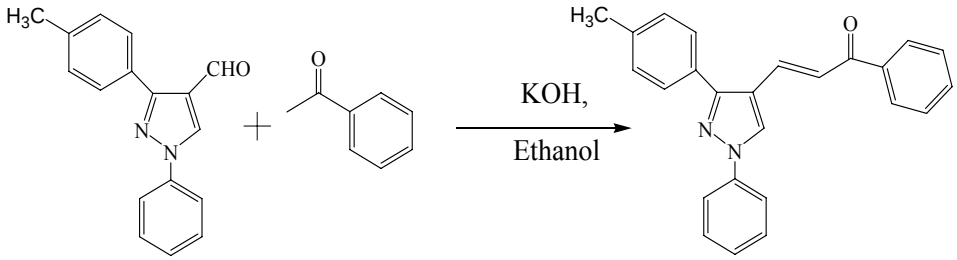

Scheme 8: synthesis of intermediate α, β unsaturated ketone **III**

1-(5-(1-phenyl-3-p-tolyl-1*H*-pyrazol-4-yl)-3-(thiophen-2-yl)-4,5-dihydropyrazol-1-yl)-ethanone (IIa)

A mixture of α,β-unsaturated ketone **II** (0.37 g, 1 mmol) and equimolar amount of hydrazine hydrate (0.048 g, 1 mmol) in glacial acetic acid (5 ml) was heated under reflux for 4 hrs. The formed white solid product was filtered, washed with ethanol, dried and recrystallized from ethanol.

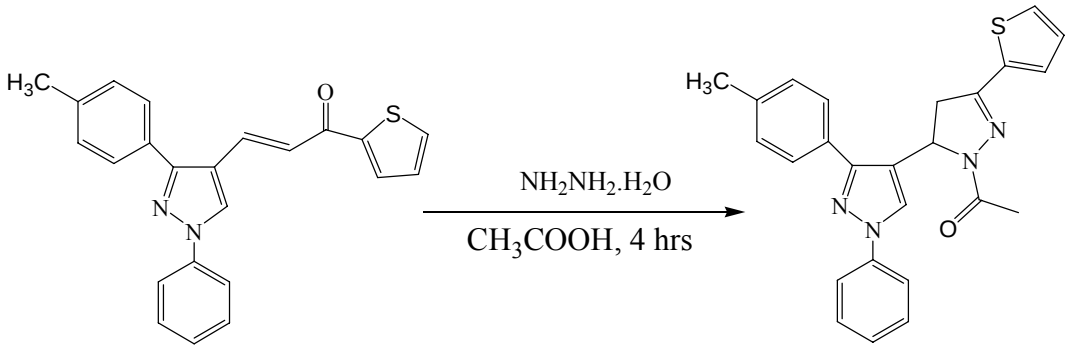

Scheme 9: Synthesis of acetyl pyrazoline derivative **IIa**

1-(3-phenyl-5-(1-phenyl-3-p-tolyl-1*H*-pyrazol-4-yl)-4,5-dihydropyrazol-1-yl)ethanone (IIIa)

A mixture of α,β-unsaturated ketone **III** (0.364 g, 1 mmol) and equimolar amount of hydrazine hydrate (0.048 g, 1 mmol) in glacial acetic acid (5 ml) was heated under reflux for 4 hrs. The formed white solid product was filtered, washed with ethanol, dried and recrystallized from ethanol/chloroform mixture (1:1).

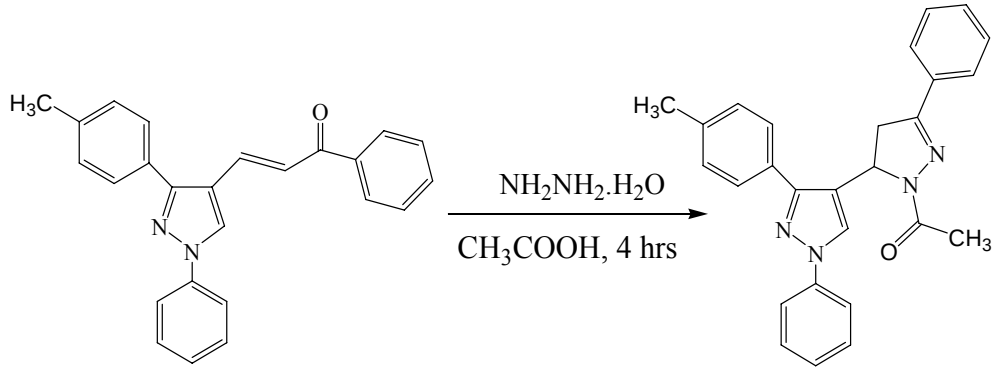

Scheme 10: Synthesis of acetyl pyrazoline derivative **IIIa**

1-(5-(1-phenyl-3-p-tolyl-1*H*-pyrazol-4-yl)-3-(thiophen-2-yl)-4,5-dihydropyrazol-1-yl)propan-1-one (IIb)

A mixture of α,β-unsaturated ketone **II** (0.37 g, 1 mmol) and equimolar amount of hydrazine hydrate (0.048 g, 1 mmol) in propionic acid (5 ml) was heated under reflux for 15 min.

The formed white solid product was filtered, washed with ethanol, dried and recrystallized from ethanol.

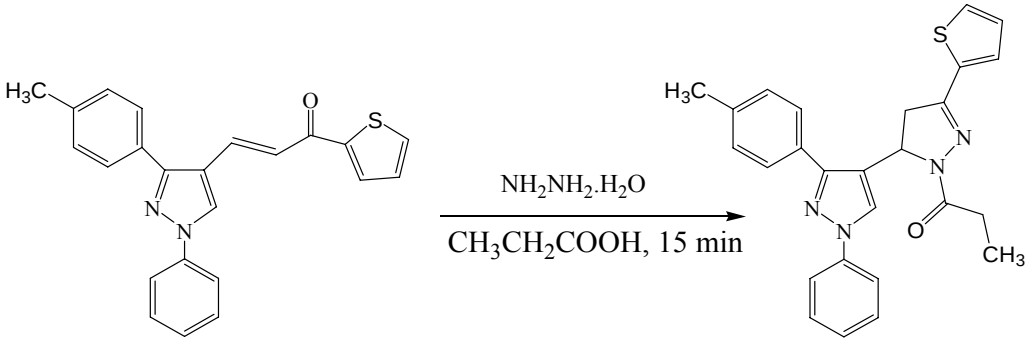

Scheme 11: Synthesis of propyl pyrazoline derivative **IIb**

1-(3-phenyl-5-(1-phenyl-3-p-tolyl-1*H*-pyrazol-4-yl)-4,5-dihydropyrazol-1-yl)propan-1-one (IIIb)

A mixture of α,β-unsaturated ketone **III** (0.364 g, 1 mmol) and equimolar amount of hydrazine hydrate (0.048 g, 1 mmol) in propionic acid (5 ml) was heated under reflux for 15 min. The obtained white solid product was filtered, washed with ethanol, dried and recrystalized from ethanol.

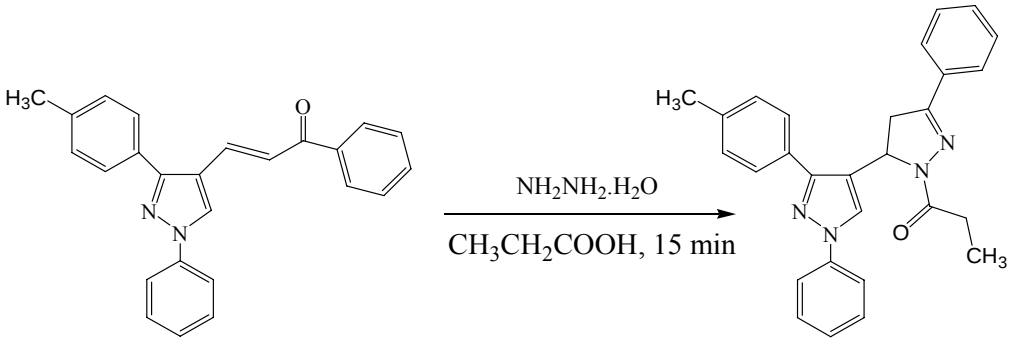

Scheme 12: Synthesis of propyl pyrazoline derivative **IIIb**

1-phenyl-4-(3-(thiophen-2-yl)-4,5-dihydro-1*H*-pyrazol-5-yl)-3-p-tolyl-1*H*-pyrazole (IIc)

A mixture of α,β-unsaturated ketone **II** (0.37 g, 1 mmol) and equimolar amount of hydrazine hydrate (0.048 g, 1 mmol) in ethanol (10 ml) was heated under reflux for 15 minutes. The separated white solid product was filtered, washed successively with water, dried and recrystalized from ethanol.

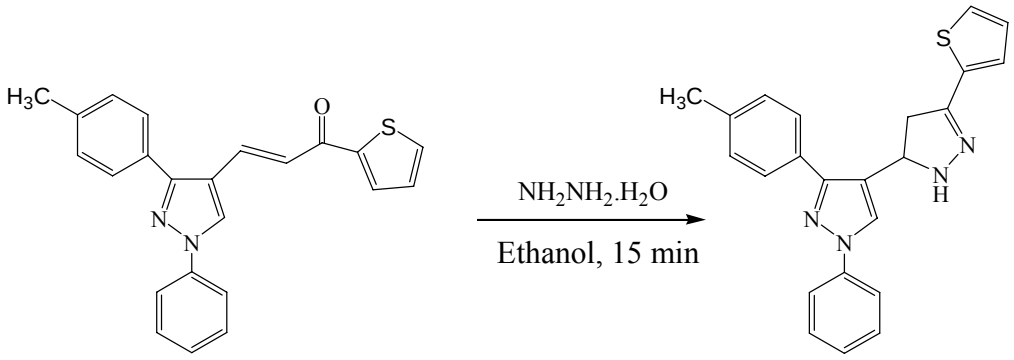

Scheme 13: Synthesis of pyrazoline derivative **IIc**

3.2.2 Determination of physical constants for the synthesized compounds

Physical constants such as percentage yield, melting point were determined. R_f values were determined on precoated silica gel of 0.25 mm thickness plates and UV-light and iodine vapor were used to visualize the spots. Ethyl acetate: n-hexane (3: 7) was used as a mobile phase to develop the chromatogram.

3.2.3 Spectroscopic analysis of the synthesized compounds

3.2.3.1 IR analysis

IR spectra of the synthesized compounds were recorded in the range of 4000-500 cm^{-1} in nujol.

3.2.3.2 ^{1}H NMR analysis

^{1}H NMR spectra were recorded using Bruker Avance DMX400 FT-NMR spectrometer operating at 400 MHz. All the compounds were dissolved in $CDCl_3$ for NMR analysis. Chemical shift values are reported in δ (ppm) using tetramethylsilane (TMS) as an internal standard.

3.2.4 Culture conditions

L. donovani was cultured in tissue flasks containing RPMI 1640 medium supplemented with 10% HIFCS and 100 IU penicillin and 100µg/ml streptomycin solution at 26 $^{\circ}$C [52, 53].

3.2.5 Stock solution and working concentration preparation

All the compounds to be tested (**II, III, IIa, IIIa, IIb, IIIb, IIc**) were dissolved in DMSO to a final concentration of 1mg/ml. Both test and standard solutions were serially diluted to appropriate concentrations using complete media. The test compounds were prepared by three fold serial dilutions from 10 µg/ml to 0.04. Amphotericin B deoxycholate and miltefosine which were used as a positive control for comparison of the antileishmanial activities of the test compounds, were also made in three fold serial dilutions [54].

3.2.6 Biological activity test

3.2.6.1 *In vivo* antimalarial activity test

The *in vivo* antimalarial activity of the synthesized compounds was determined by standard 4 day suppressive test using *P. berghei* ANKA strain infected mice as described by David, *et al*. [55]. This test is the most widely used preliminary test by which activity of various compounds is assessed by comparison of blood parasitemia and mouse survival time in treated and untreated mice [56]. Accordingly, test mice were infected with 0.2 ml of $2X10^7$ parasitized erythrocytes (*P. berghei* ANKA strain) intraperitonialy on day 0. These parasitized erythrocytes were obtained from the blood of a donor mouse with 27% parasitemia which was then diluted with normal saline (1:4).

Mice were then weighed and randomly divided into nine groups of five mice per cage 2 hr after infection. The first seven groups received the synthesized compounds suspended in a vehicle containing 7% Tween and 3% ethanol in water orally, at 48.46 µmol/kg dose level. Group eight received the vehicle only and acted as a negative control. The Standard drug, chloroquine phosphate dissolved in the same solvent, was administered orally at a dose of 48.4 µmol/kg to mice in group nine and served as positive control [57, 58].

On days 1 to 3 (24 hr time interval on successive dosing), animals in test groups were treated again with the same dose of the synthesized compounds through the same route as in day 0. On day 4 that is 24 hr after the last dose or 96 hr post-infection, the mice were weighed and blood smear was prepared on slides. The blood was then fixed with absolute methanol and stained with Giemsa stain. Level of parasitemia was determined microscopically by counting 4 fields of approximately 100 erythrocytes per field. The difference between the mean

parasitemia level of the negative control group (taken as 100%) and that of test compound treated group was calculated and expressed as percent suppression. The survival time for each test mouse was recorded except for chloroquine treated ones which were completely cured of the parasite [58].

Percent parasitemia and percent suppression was calculated using the following two formulas

$$\% \text{ parasitemia} = \frac{\text{Number of infected RBC}}{\text{Number of total RBC}} \times 100$$

$$\% \text{ Suppression} = \frac{\text{Parasitemia in negative control - parasitemia in study group}}{\text{parasitemia in negative control}} \times 100$$

#

3.2.6.2 *In vitro* antipromastigote assay

Promastigote forms of *L. donovani* and standard drugs of amphotericin B deoxycholate and miltefosine were used for the assay. 3x 10^6 promastigotes of *L. donovani* in 100 µl were seeded to each well in a 96 well flat bottom plate. Various dilutions of test compounds (10, 3.33, 1.11, 0.37, 0.12, 0.04 µg/ml) were added to the parasites. The tests were done in duplicates. Some of the wells contained only the standard drugs and served as a positive control. The media and DMSO alone were used as a negative control. The plates were then kept at room temperature. After 24 hr, 20 µl of alamar blue (12.5 mg resazurin dissolved in 100 ml of distilled water) [59] was added to each of the wells. Absorbance of the resulting mixture was measured after 48 hr at a wavelength of 540 and 630 nm using Enzyme Linked Immuno Sorbent Assay (ELISA) plate reader [60].

A quantitative colorimetric assay using the oxidation-reduction indicator Alamar Blue was developed to measure cytotoxicity of the synthesized compounds against the protozoan parasite *Leishmania donovani*. The Alamar Blue assay permits a simple, reproducible and reliable method for screening antileishmanial drugs [61, 62].

Alamar blue reduction assay is considered to be better than all the other methods as it is easy, rapid, sensitive and cost effective for continuous monitoring of cell cultures. The redox indicator alamar blue is water soluble, non toxic to cells and highly stable in complete media so that it is widely used for quantification of viability of leishmania and various other cells *in vitro* [63].

AlamarBlue® works as a cell viability and proliferation indicator through the conversion of Resazurin (blue and nonfluorescent), to resorufin (pink and highly fluorescent) and further to hydroresorufin (uncoloured and nonfluorescent) through reduction reactions of metabolically active cells, Figure 14. The amount of fluorescence produced is proportional to the number of living cells [62].

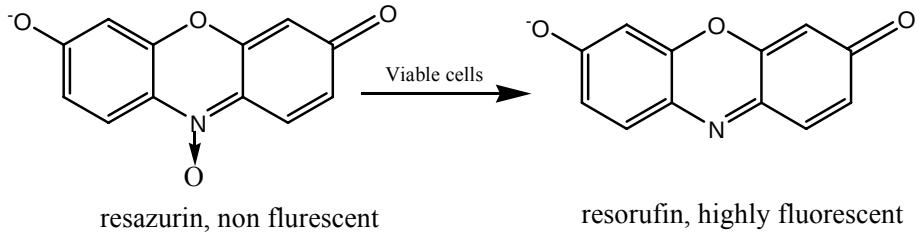

Figure 17: Conversion of resazurin into resorufin by metabolically active cells

3.2.7 Data analysis

Results of the antimalarial activity test were expressed as mean ± standard deviation. Statistical significance for suppressive test was determined by one-way ANOVA. All data were analyzed at 95% confidence limits (p=0.05). The IC_{50} values for synthesized compounds tested for their *in vitro* antileishmanial activity were evaluated from sigmoidal dose- response curves using non linear regression software (GraphPad Prism®; GraphPad Software, Inc., San Diego, CA)

4 RESULTS AND DISCUSSION

4.1 Synthesis of target compounds

4.1.1 Synthesis of the intermediate compound

The intermediate α, β-unsaturated ketone compounds **II** and **III** were synthesized by applying aldol condensation. Aldol condensation reaction involves nucleophilic addition of a ketone enolate to an aldehyde. The aldol product, when loses a molecule of water, the corresponding α,β-unsaturated ketone is formed. A strong base, potassium hydroxide was used as a catalyst to produce ketone enolate.

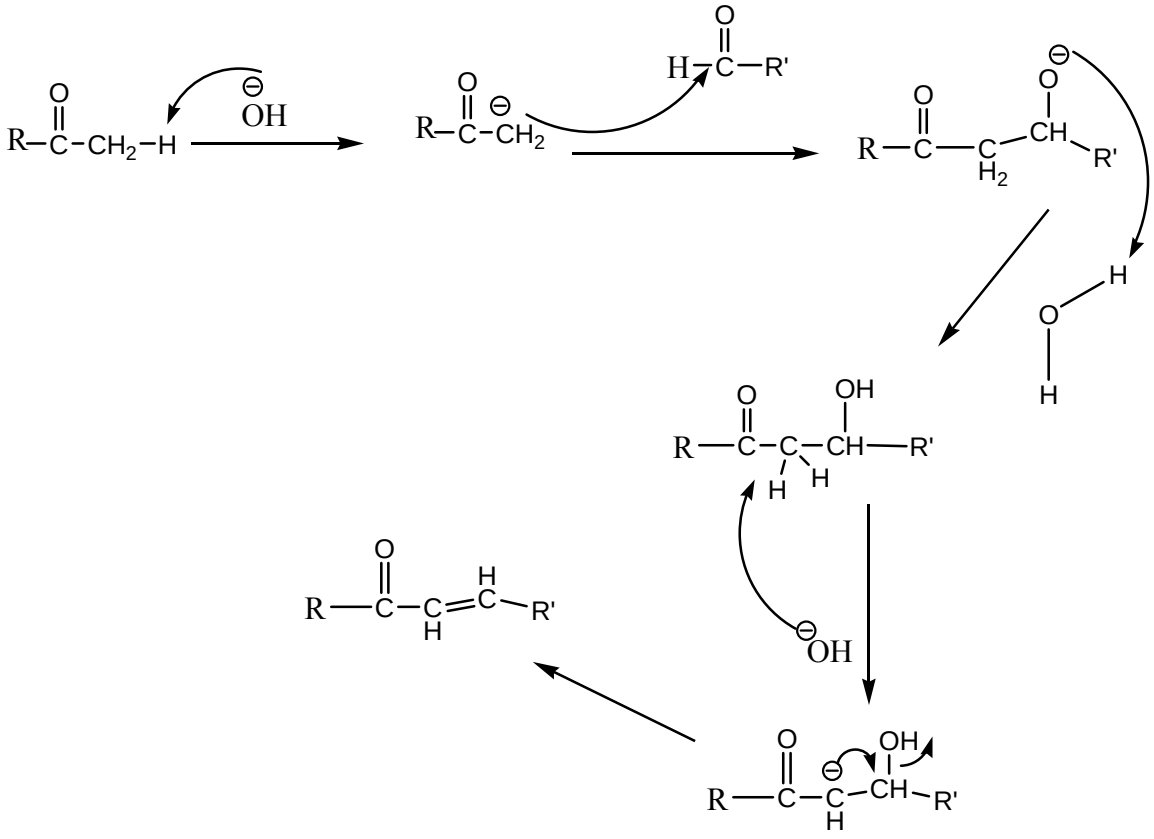

Scheme 14: Mechanism for α,β-unsaturated ketone formation

4.1.2 Synthesis of thienyl and phenyl pyrazoline derivatives

The pyrazoline derivatives were obtained via Michael type addition. The compounds were synthesized by nucleophilic attack of hydrazine hydrate on the α,β-unsaturated ketone followed by cyclisation.

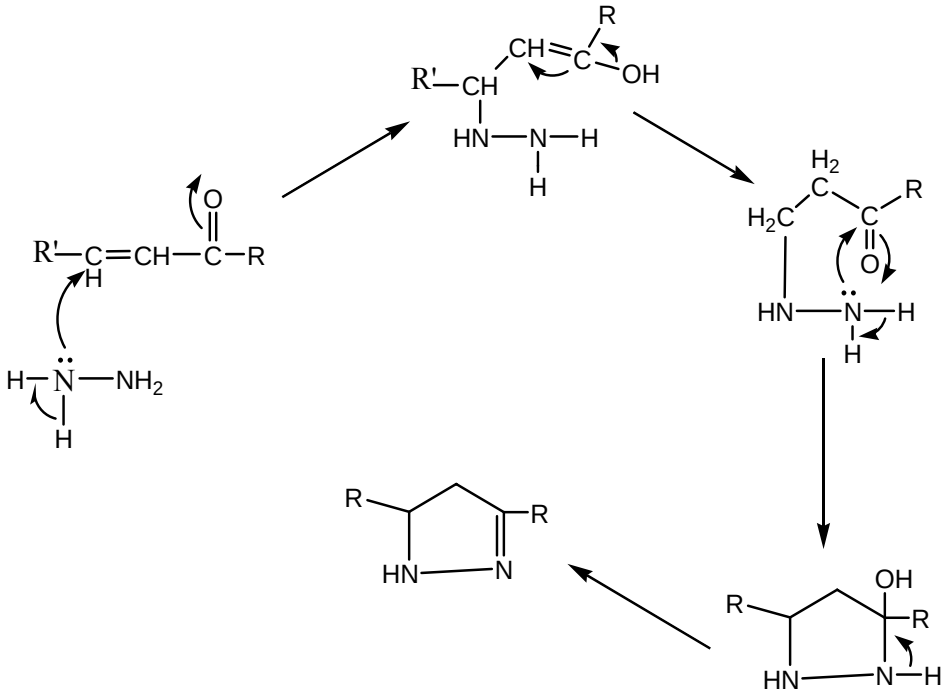

Scheme 15: Mechanism for pyrazoline formation

4.2 Physical properties, percentage yield and elemental microanalysis

TLC was used to monitor the progress of chemical reactions and confirm their completion. The purity of the synthesized compounds was also inferred on TLC from one spot for each target compound in three different developing solvents. Percentage yield, R_f values, melting point and elemental microanalyses of the synthesized compounds were determined. As shown in table 1, compound **IIIa** was produced in the highest yield (95.23%) while the least percentage yield was observed for compound **IIc** (71.39%). All the synthesized compounds

were completely soluble in chloroform. Elemental microanalyses were also performed to find out their C, H, N, and S percentage composition. The results obtained were found to be within ± 0.4% of the theoretical values. This was done to assure the formation and purity of the proposed compounds. The results obtained are illustrated in table 1.

Table 1: Results for physical and elemental microanalyses of the synthesized compounds

Comp. №	**Yield %**	**M.P. (C^o)**	**Rf. value**	**Mol.Formula (Mol.wt.)**	**Elemental analysis %, Cald/*Found***			
					C %	**H %**	**N %**	**S %**
II	90.0	203-204	0.62	$C_{23}H_{18}N_2OS$ (370.47)	**74.53** *74.58*	**4.90** *5.21*	**7.56** *7.70*	**8.66** *8.34*
III	86.0	173-174	0.71	$C_{25}H_{20}N_2O$ (364.44)	**82.39** *82.18*	**5.53** *5.74*	**7.69** *7.46*	
IIa	85.3	193-194	0.67	$C_{25}H_{22}N_4OS$ (426.53)	**70.40** *69.95*	**5.20** *5.35*	**13.14** ***13.27***	**7.52** *7.72*
IIIa	95.2	219-220	0.53	$C_{27}H_{24}N_4O$ (420.51)	**77.12** *76.89*	**5.75** *5.71*	**13.32** *13.48*	
IIb	75.0	204-205	0.48	$C_{26}H_{24}N_4OS$ (440.56)	**70.88** *71.11*	**5.49** *5.72*	**12.72** *12.92*	**7.28** *7.54*
IIIb	82.0	200-201	0.66	$C_{28}H_{26}N_4O$ (434.53)	**77.39** *77.21*	**6.03** *5.87*	**12.89** *12.78*	
IIc	71.4	119-120	0.75	$C_{23}H_{20}N_4S$ (384.5)	**71.87** *72.06*	**5.24** *5.57*	**14.57** *14.34*	**8.34** *8.62*

4.3 Spectral analysis of the synthesized compounds.

Spectral analysis such as IR and ^{1}H NMR were done to confirm the presumed structures of the synthesized compounds. All the functional groups and protons were observed at the expected values.

(E)-3-(1-phenyl-3-p-tolyl-1*H*-pyrazol-4-yl)-1-(thiophen-2-yl)-prop-2-en-1-one (II)

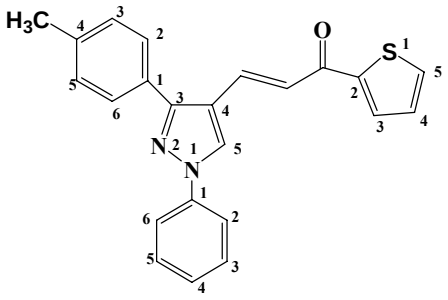

IR (nujol) cm^{-1}: 1636 (C=O); 1563 (C=N).

^{1}H NMR ($CDCl_3$/ CCl_4): δ (ppm) ; 2.45 (s, 3H, phenyl-CH_3), 7.17-7.40 (m, 5H, C<u>H</u>=CH-CO, phenyl-$C_{3,4,5}$H, thiophen- C_4 H), 7.45-7.53 (m, 2H, phenyl-$C_{2,6}$H), 7.60 (d, 2H, J= 8.27 Hz, *p*- tolyl-$C_{3,5}$ H), 7.65 (d, 1H, J= 5.96 Hz, thiophen-C_3 H), 7.75 (d, 1H, J= 4.85 Hz, thiophen-C_5 H), 7.80 (d, 2H, J= 8.27 Hz, *p*-tolyl-$C_{2,6}$ H), 7.92 (d, 1H, J= 15.6 Hz, CH=C<u>H</u>-CO), 8.36 (s, 1H, pyrazole-C_5 H). Anal. Calcd for $C_{23}H_{18}N_2OS$: C, 74.53; H, 4.90; N, 7.56. Found C, **74.58**; H, **5.21**; N, **7.70**.

The IR spectrum of compound **II** is shown in figure **5**. The carbonyl stretching band was observed at a low frequency of 1636 cm^{-1} because of the resonance effect induced by conjugation with a double bond. The -C=N- stretching band was observed at 1563 cm^{-1}.

The ^{1}H NMR spectrum of compound **II** is presented in figure **6**. The upfield singlet peak observed at 2.45 ppm and integrated for 3 protons is attributed to the methyl group. The doublet at 7.92 ppm, integrated to one proton is attributed to the vinyl proton. The J value, 15.6Hz confirms trans configuration of the vinyl protons. The peak for C<u>H</u>=CH-CO is deshielded due to conjugation to the electron withdrawing carbonyl group. The multiplet at 7.17-7.40 ppm and integrated for 5 protons is attributed to the CH=C<u>H</u>-CO, N_1-phenyl-$C_{3,4,5}$H and thiophen C_4-H. The expected doublet peak for CH=C<u>H</u>-CO is overlaped with the multiplet peak. The multiplet at 7.45-7.53 ppm integrated to two protons and attributed to the N1-phenyl-$C_{2,6}$H is deshielded due to effect of the pyrazole nitrogen. The two doublets at 7.60 and 7.80 ppm each integrated for two protons are attributed to *p*- tolyl-$C_{3,5}$ H and *p*-tolyl-$C_{2,6}$ H respectively. The peak for *p*-tolyl-$C_{2,6}$ H is more deshielded because of its proximity to the electron withdrawing effect of the pyrazole ring. The two doublets at 7.65 and 7.75 ppm each integrated for one proton are attributed to the thiophen-C_3 and C_5 protons. The characteristic singlet peak for pyrazole-C_5 H appeared at the most deshielded position 8.36 ppm because it is near to the electron withdrawing effect of the pyrazole nitrogen. The absence of the characterstic aldehydic singlet peak of the starting material around 10.0 ppm further confirmed the formation of compound **II**.

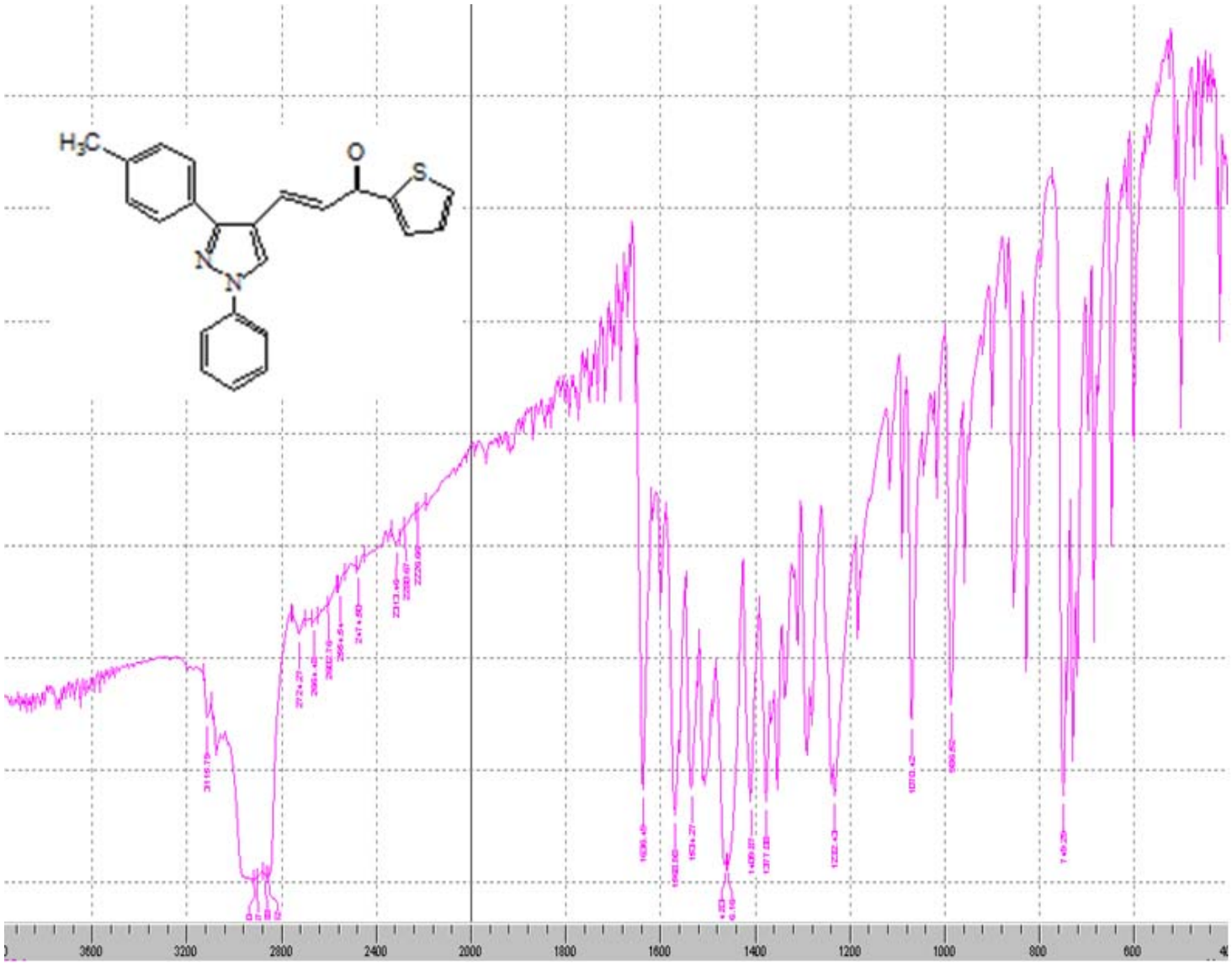

Figure 5: IR spectrum of compound **II** in nujol

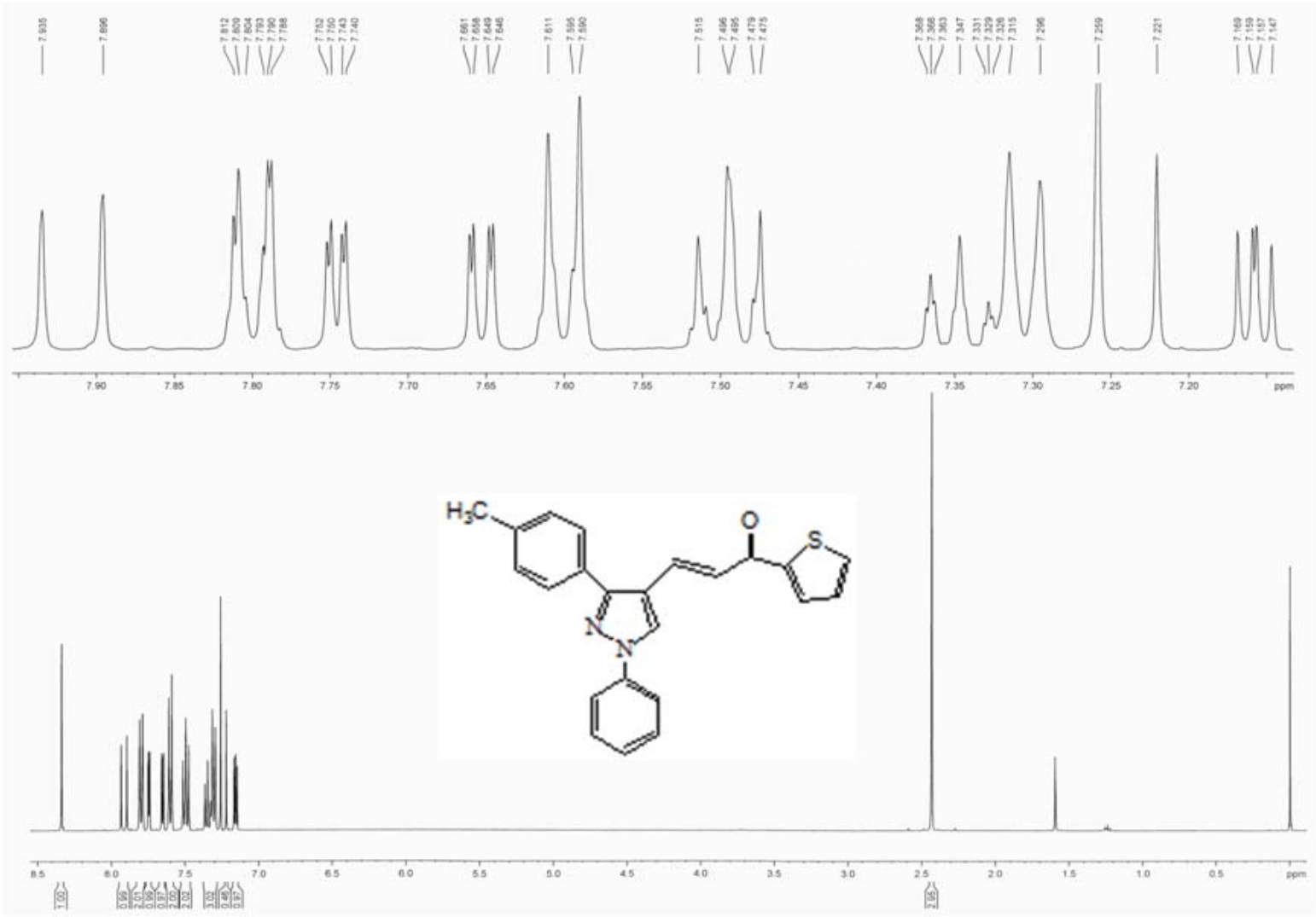

Figure 6: ^{1}H NMR spectrum of compound **II** in $CDCl_3$

(E)-1-phenyl-3-(1-phenyl-3-p-tolyl-1*H*-pyrazol-4-yl)-prop-2-en-1-one (III)

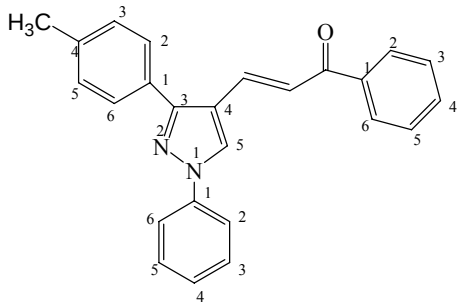

IR (nujol) cm^{-1}: 1645 (C=O); 1595 (C=N).

^{1}H NMR ($CDCl_3$/ CCl_4): δ (ppm) ; 2.45 (s, 3H, phenyl-CH_3), 7.28-7.38 (m, 4H, C<u>H</u>=CH-CO, N_1-phenyl-$C_{3,4,5}$H), 7.45-7.51 (m, 4H, *p*-tolyl-$C_{2,3,5,6}$ H), 7.53-7.61 (m, 3H, carbonyl-phenyl-$C_{3,4,5}$H), 7.79 (d, 2H, J=7.56Hz, N_1-phenyl-$C_{2,6}$), 7.89 (d, 1H, J=15.67Hz, CH=C<u>H</u>-CO), 7.96 (d, 2H, J=7.06Hz, carbonyl-phenyl-$C_{2,6}$H), 8.36 (s, 1H, pyrazol-C_5H). Anal. Calcd for $C_{25}H_{20}N_2O$: C, 82.39; H, 5.53; N, 7.69. Found C, **82.18**; H, **5.74**; N, **7.46**.

The IR spectrum of compound **III** is shown in figure **7**. The carbonyl stretching band was observed at a low frequency of 1645 cm^{-1} due to the resonance induced by conjugation the double bond. The -C=N- stretching band was observed at 1595 cm^{-1}.

The ^{1}H NMR spectrum of compound **III** is presented in figure **8**. The multiplet peak at 7.28-7.38 ppm and integrated for 4 protons is attributed to CH=C<u>H</u>-CO and N_1-phenyl-$C_{3,4,5}$H protons. The expected doublet peak to CH=C<u>H</u>-CO is overlapped with the multiplet peak for N_1-phenyl-$C_{3,4,5}$H protons. The other multiplet peak integrated for three protons at 7.53-7.61ppm is attributed to carbonyl-phenyl-$C_{3,4,5}$H and it is more deshielded due to the stronger electron withdrawing effect of the carbonyl group. The two doublets at 7.79 and 7.96 ppm

are attributed to N_1-phenyl-$C_{2,6}$H and carbonyl-phenyl-$C_{2,6}$H protons respectively, the latter being more deshielded due to the stronger electron withdrawing effect of the carbonyl group than the pyrazole N_1. The characteristic singlet peak for pyrazole-C_5 H appeared at the most deshielded position 8.36 ppm because it is near to the electron withdrawing effect of the pyrazole nitrogen. The absence of characteristic aldehydic singlet peak of the starting material around 10.0 ppm confirmed the formation of compound **III**.

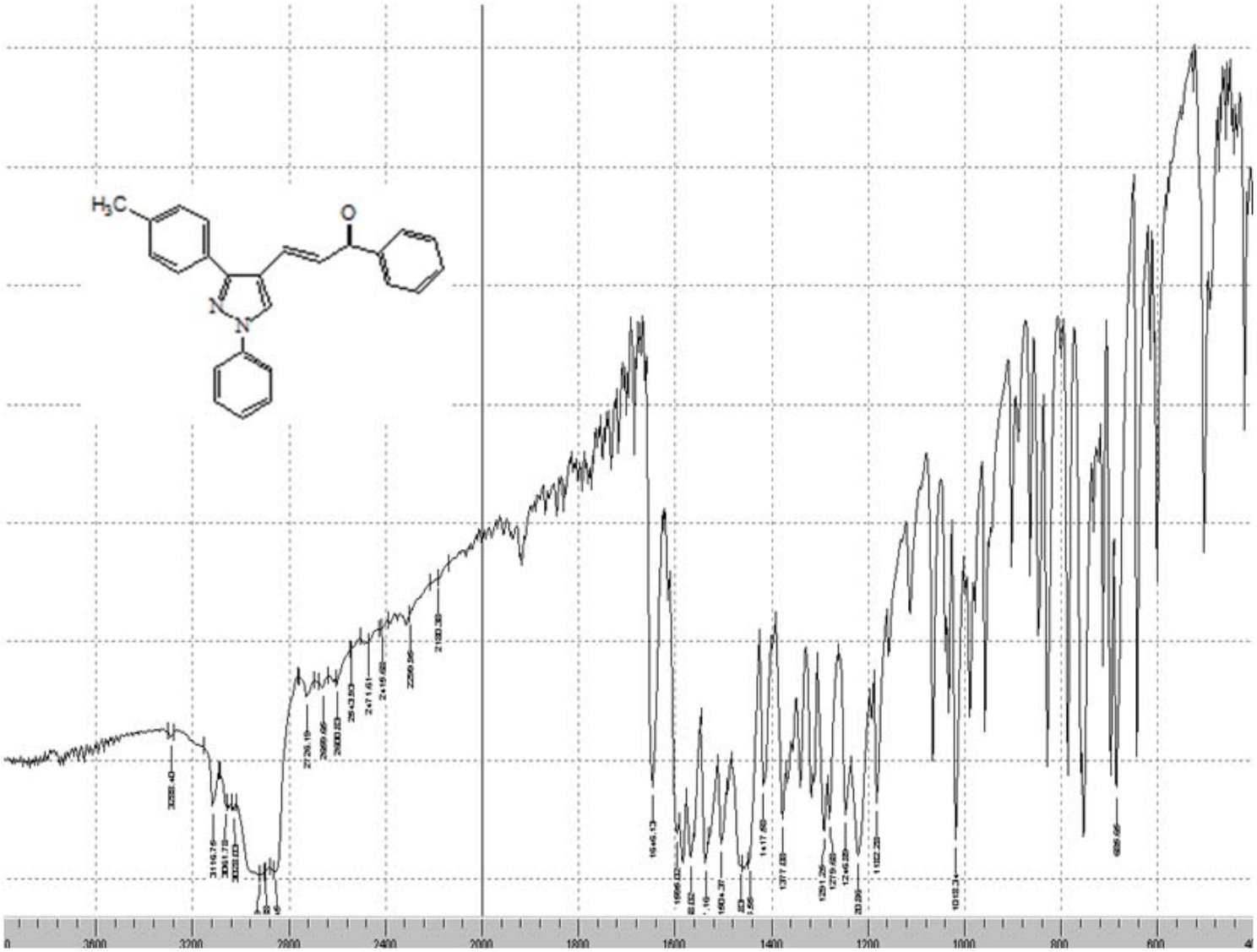

Figure 7 : IR spectrum of compound **III** in nujol

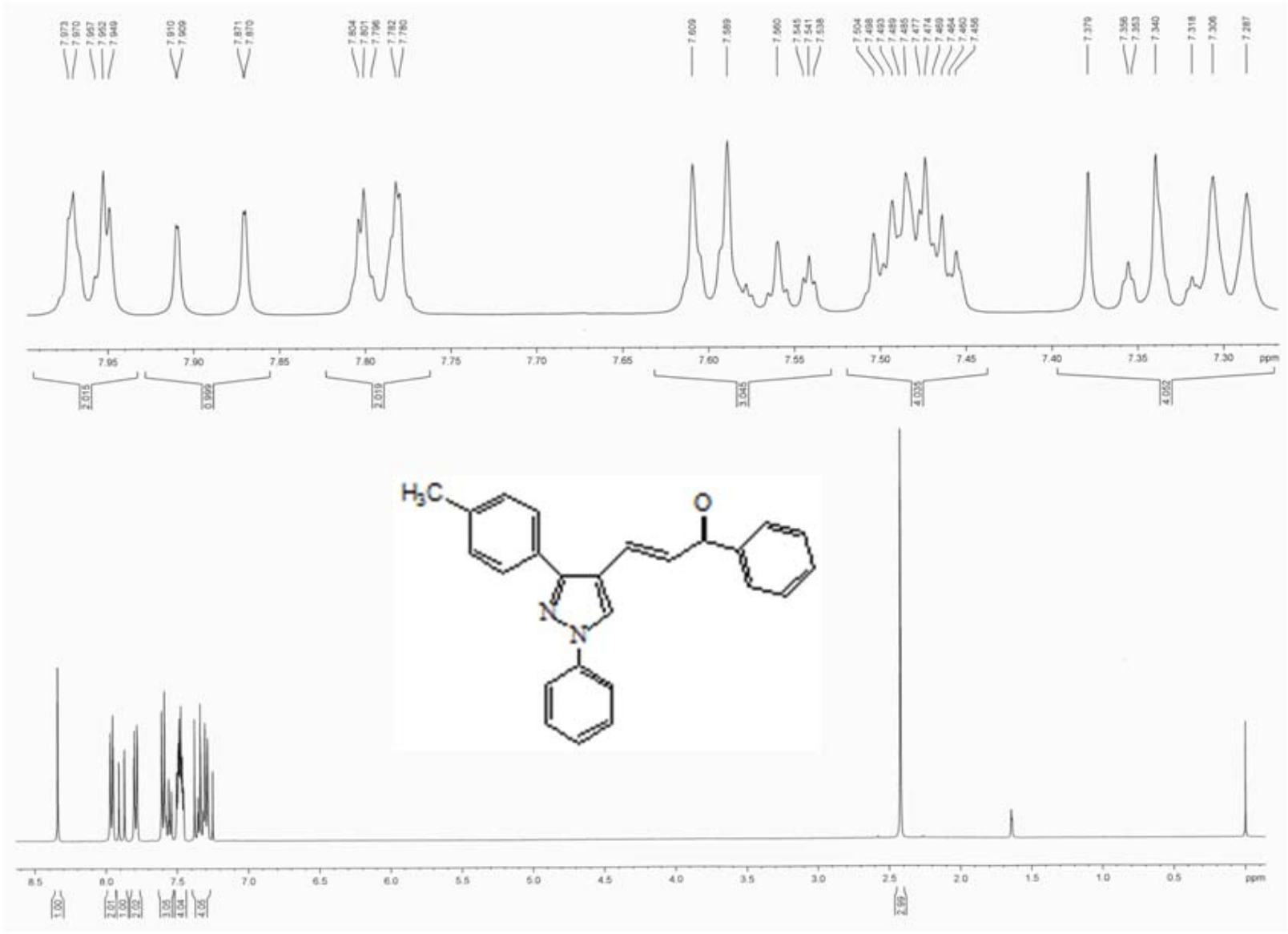

Figure 8: ^{1}H NMR spectrum of compound **III** in $CDCl_3$

1-(5-(1-phenyl-3-p-tolyl-1*H*-pyrazol-4-yl)-3-(thiophen-2-yl)-4,5-dihydropyrazol-1-yl)-ethanone (IIa)

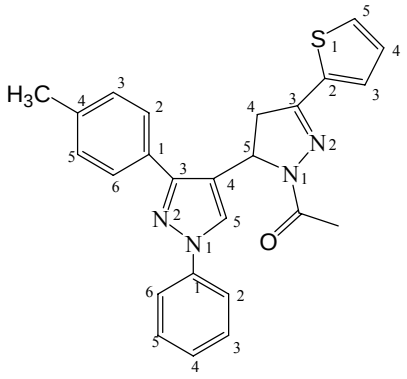

IR (nujol) cm^{-1}: 1658 (C=O); 1600 (C=N).

NMR ($CDCl_3$/ CCl_4): δ (ppm) ; 2.40 (s, 3H, phenyl-CH_3), 2.45 (s, 3H, $COCH_3$), 3.09 (dd, 1H, J=4.4Hz, pyrazoline-C_4H), 3.65 (dd, 1H, J= 11.5Hz, pyrazoline-C_4H), 5.91 (dd, 1H, J=4.36Hz, pyrazoline-C_5 H), 7.05 (dd, 1H, thiophene-C_4), 7.13 (d, 1H, J=2.8Hz, thiophene-C_3H), 7.26-7.3 (m, 3H, N_1-phenyl-$C_{3,4,5}H$), 7.4-7.5 (m, 3H, thiophene-C_5H, N_1-Phenyl-$C_{2,6}H$), 7.66 (d, 2H, J=7.83Hz, *p*- tolyl-$C_{3,5}$ H), 7.71 (d, 2H, J=7.83Hz, p-tolyl-$C_{2,6}H$), 7.8 (s, 1H, pyrazole-C_5H). Anal. Calcd for $C_{25}H_{22}N_4OS$: C, 70.40; H, 5.20; N, 13.14. Found C, **69.95**; H, **5.35**; N, **13.27**.

The IR spectrum of compound **IIa** is shown in figure **9**. The shift of the carbonyl stretching band relative to the starting material (the compound **II)** to a higher frequency of 1658 cm^{-1} confirms the absence of conjugation to a double bond. However, this band appeared at low frequency as it is amidic carbonyl group.

The ^{1}H NMR of compound **IIa** is shown in figure **10.** The two singlet peaks at 2.40 and 2.45 ppm each integrated for three protons are attributed to phenyl-CH_3 and $COCH_3$ respectively. The latter is more deshielded due to the electron withdrawing efffect of the carbonyl group. The two doublet of doublet peaks at 3.09 ppm and 3.65 pm each integrated for one proton are attributed to pyrazoline C_4-H. Another doublet of doublet peak at 5.91 ppm integrated for one proton and attributed to pyrazoline C_5-H was also observed. These are characteristic peaks that confirmed the formation of the pyrazoline ring. The peak due to pyrazoline C_5-H appears relatively more deshielded because of the presence of adjacent pyrazole ring. The triplet peak at 7.05 ppm is attributed to thiophene C_4-H. The doublets at 7.66 and 7.71 ppm, integrated for two protons each are attributed to p-tolyl $C_{3,5}$ and $C_{2,6}$ protons, respectively. The peak for *p*-tolyl $C_{2,6}$-H is more deshielded since it is relatively closer to the electron withdrawing pyrazole ring. The characteristic singlet for pyrazole-C_5 H appeared at the most deshielded position 7.8 ppm.

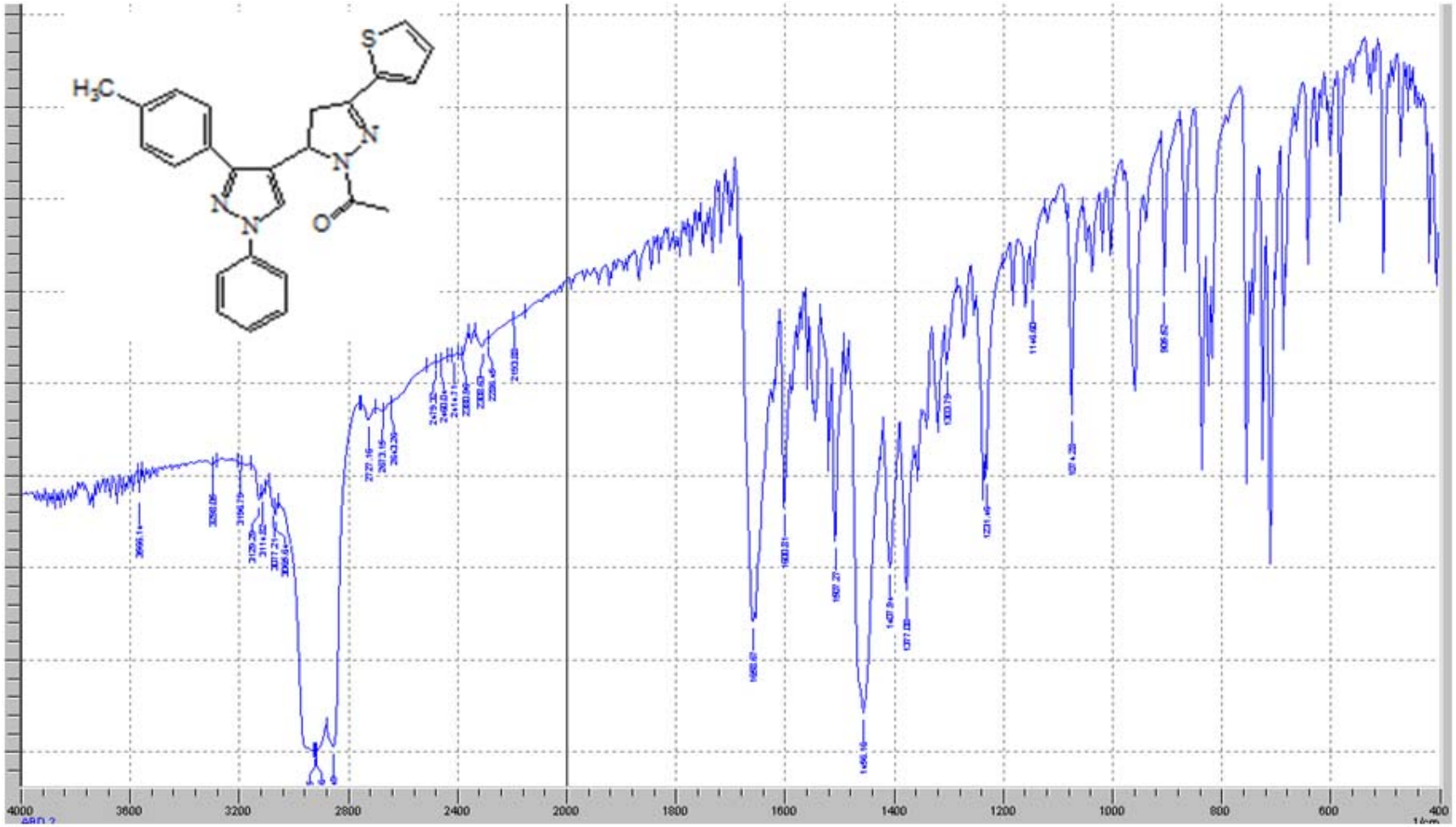

Figure 9: IR spectrum of compound **IIa** in nujol

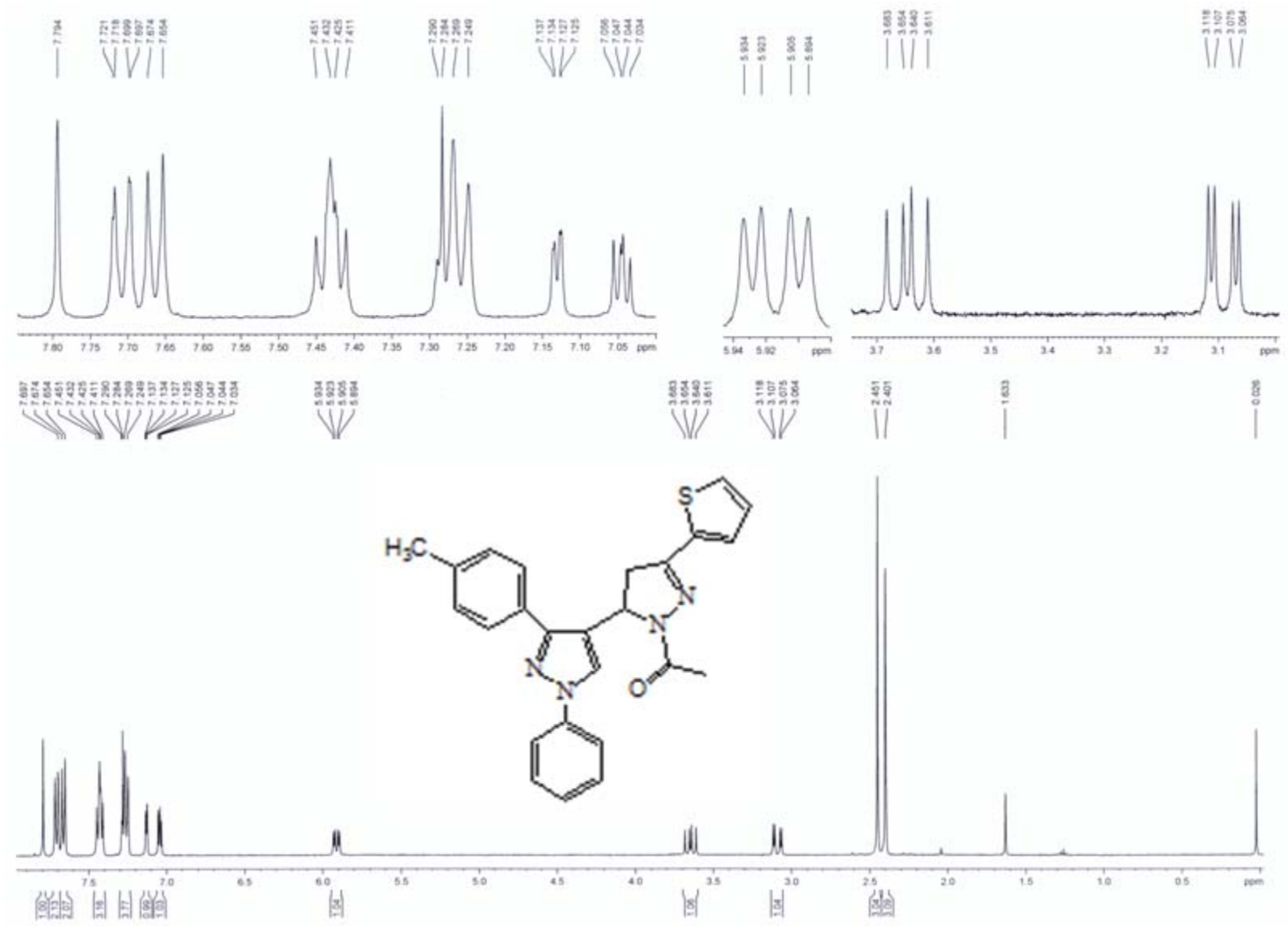

Figure 10: ^{1}H NMR spectrum of compound **IIa** in $CDCl_3$

1-(3-phenyl-5-(1-phenyl-3-p-tolyl-1*H*-pyrazol-4-yl)-4,5-dihydropyrazol-1-yl)ethanone (IIIa)

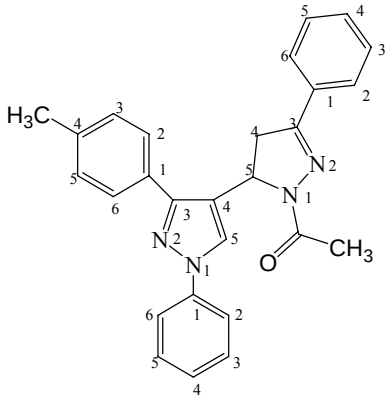

IR (nujol) cm^{-1}: 1652 (C=O); 1594 (C=N).

^1H NMR ($CDCl_3$/ CCl_4): δ (ppm) ; 2.38 (s, 3H, phenyl-CH_3), 2.5 (s, 3H, $C\underline{H}_3CO$), 3.12 (dd, 1H, J= 4.40 Hz, pyrazoline-C_4 H), 3.64 (dd, 1H, J= 11.6 Hz, pyrazoline-C_4 H), 5.95 (dd, 1H, J= 4.4, 11.6 Hz, pyrazoline-C_5 H), 7.26 (t, 3H, phenyl-$C_{3,4,5}$H), 7.38-7.46 (m, 5H, N_1-phenyl-H), 7.65-7.72 (m, 6H, phenyl-$C_{2,6}$H, p-tolyl-$C_{2,3,5,6}$H), 7.8 (s, 1H, pyrazole-C_5H). Anal. Calcd for $C_{27}H_{24}N_4O$: C, 77.17; H, 5.75; N, 13.32. Found C, **76.89**; H, **5.71**; N, **13.48**.

The IR spectrum of compound **IIIa** is shown in figure **11**. The shift of the carbonyl stretching band relative to compound **III** to a higher frequency of 1652 cm^{-1} confirms the absence of conjugation to a double bond. This band appeared at low frequency as it is amidic. The C=N stretching band was observed at 1594 cm^{-1}.

The ^1H NMR of compound **IIIa** is shown in figure **12**. The two singlet peaks at 2.38 and 2.50 ppm each integrated for three protons are attributed to phenyl-CH_3 and $COCH_3$ respectively. The latter peak is more deshielded due to the electron withdrawing efffect of the carbonyl group. Characterstic peaks that indicate the formation of pyrazoline moiety, as described in

compound **IIa**, are also observed. A triplet peak integrated for three protons of phenyl-$C_{3,4,5}H$ is observed at 7.26 ppm. Two multiplet peaks at 7.38-7.46 ppm and 7.65-7.72 ppm integrated for five and six protons respectively were attributed to the N_1-phenyl-H, and phenyl-$C_{2,6}H$, p-tolyl-$C_{2,3,5,6}H$ protons respectively. The other characteristic peak is the singlet integrated for one proton at 7.8 ppm which is attributed to pyrazole-C_5 H.

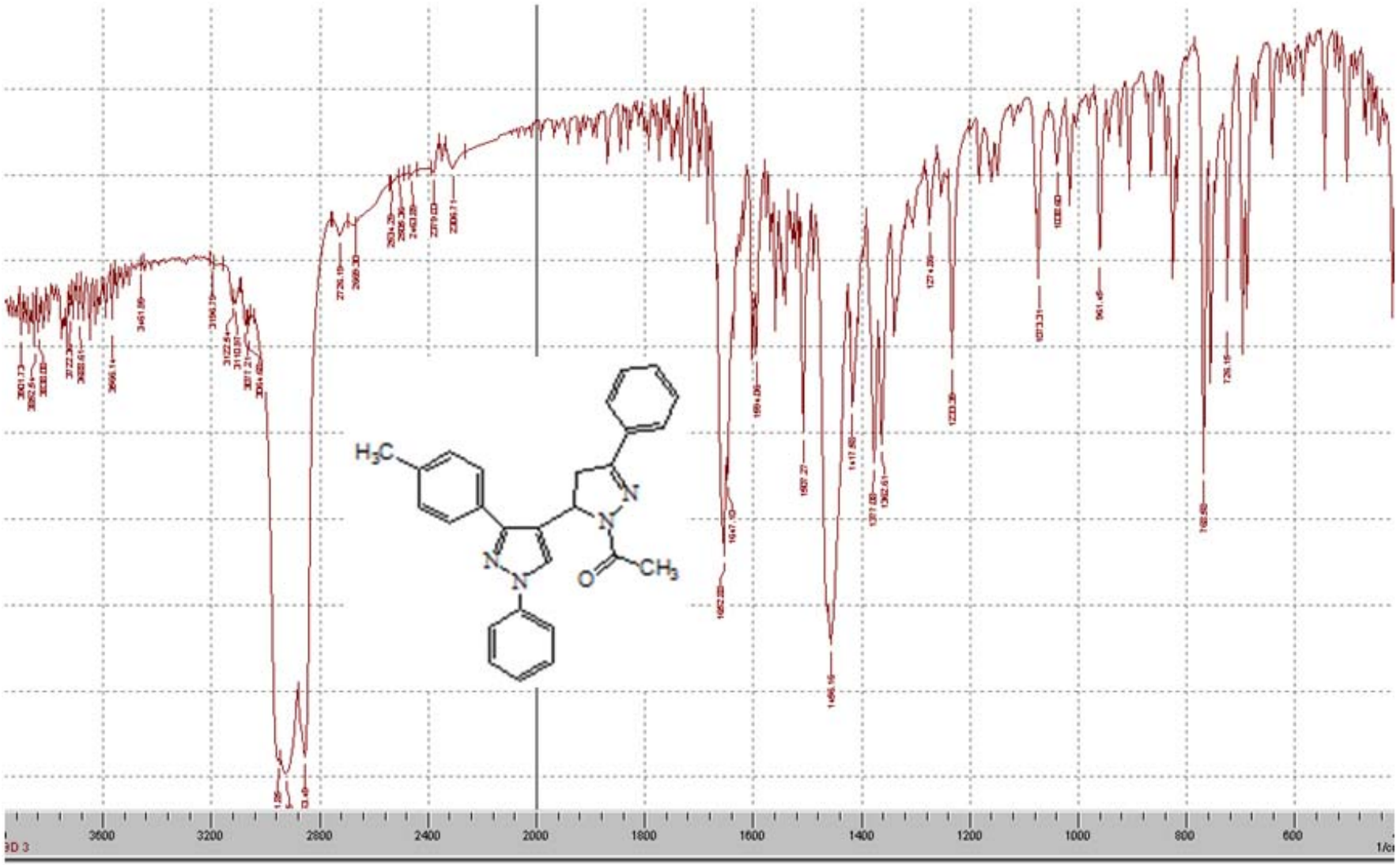

Figure 11: IR spectrum of compound **IIIa** in nujol

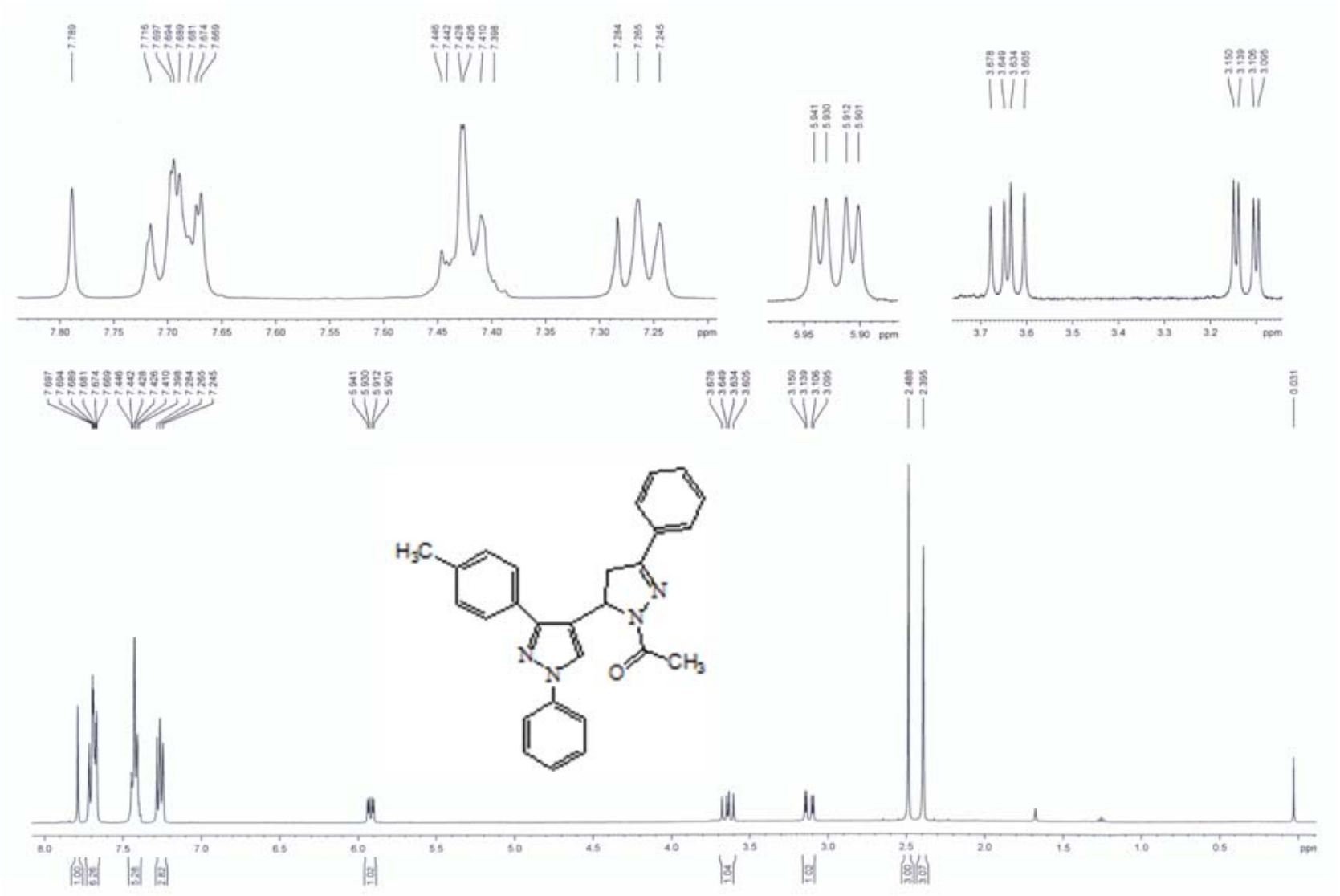

Figure 12: ^{1}H NMR spectrum of compound **IIIa** in $CDCl_3$

1-(5-(1-phenyl-3-p-tolyl-1*H*-pyrazol-4-yl)-3-(thiophen-2-yl)-4,5-dihydropyrazol-1-yl)propan-1-one (IIb)

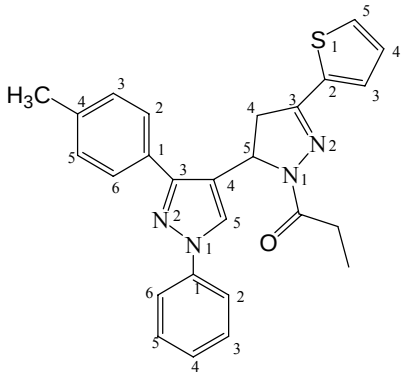

IR (nujol) cm^{-1}: 1640 (C=O); 1600 (C=N).

^{1}H NMR ($CDCl_3$/ CCl_4): δ (ppm) ; 1.23 (t, 3H, J= 7.5Hz, C<u>H</u>$_3$-CH_2), 2.38 (s, 3H, tolyl-CH_3), 2.82 (q, 2H, J= 7.5Hz, CH_3C<u>H</u>$_2$), 3.05 (dd, 1H, J= 4.3Hz, pyrazoline-C_4 H), 3.60 (dd, 1H, J= 11.6Hz, pyrazoline-C_4 H), 5.88 (dd, 1H, J= 4.3, 11.6Hz, pyrazoline-C_5 H), 7.02 (t, 1H, thiophen-C_4H), 7.10 (d, 1H, J=3.59Hz, thiophen-C_5H), 7.23 (m, 3H, thiophen-C_3H, p-tolyl-$C_{3,5}$H), 7.38-7.43 (m, 3H, N_1-phenyl-$C_{3,4,5}$H), 7.63 (d, 2H, J=7.69Hz, N_1-phenyl-$C_{2,6}$H), 7.69 (d, 2H, p-tolyl-$C_{2,6}$H), 7.8 (s, 1H, pyrazole-C_5H). Anal. Calcd for $C_{26}H_{24}N_4OS$: C, 70.88; H, 5.49; N, 12.72. Found C, **71.11**; H, **5.72**; N, **12.92**.

The IR spectrum of compound **IIb** is given in figure **13**. Characteristic band was observed at 1640 cm^{-1} which was attributed to C=O stretching vibration. The band occurred at a low frequency as it is amidic group.

The ^{1}H NMR of compound **IIb** is shown in figure**14**. Peaks that confirm presence of propanoyl protons were observed. The triplet and quartet peaks at 1.23 and 2.82 ppm, integrated for three and two protons, respectively are indicated to C<u>H</u>$_3$-CH_2 and CH_3C<u>H</u>$_2$

`respectively. The quartet peak is more deshielded as the two protons are nearer to the electron withdrawing carbonyl group. The two doublet of doublets (integrated for one proton each) at 3.05 ppm and 3.60 ppm are attributed to pyrazoline-C_4 H. The other doublet of doublets that was observed at 5.88 ppm, integrated for one proton, is attributed to pyrazoline-C_5 H. This proton at C_5 of pyrazoline ring is relatively more deshielded because of the presence of adjacent pyrazole ring. The appearance of these three doublets of doublet peaks confirmed formation of the pyrazoline ring. The triplet peak at 7.02 ppm integrated for a single proton is attributed to thiophen C_4-H. The two doublets at 7.63 ppm and 7.69 ppm, each integrated for two protons, are attributed to N_1-phenyl-$C_{2,6}$H and p-tolyl-$C_{2,6}$H. The most deshielded singlet at 7.80 ppm is attributed to pyrazole-C_5 H.

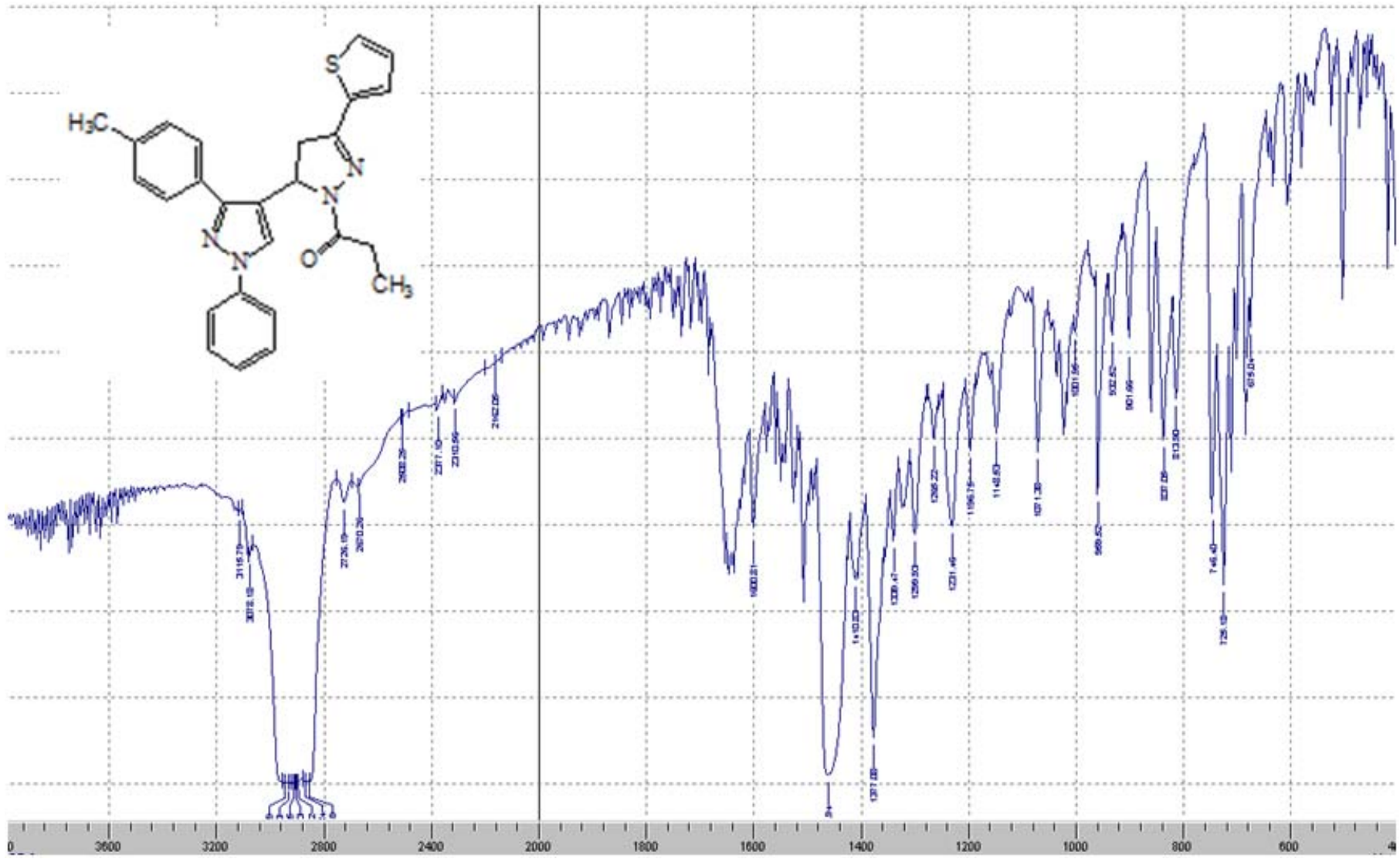

Figure 13: IR spectrum of compound **IIb** in nujol

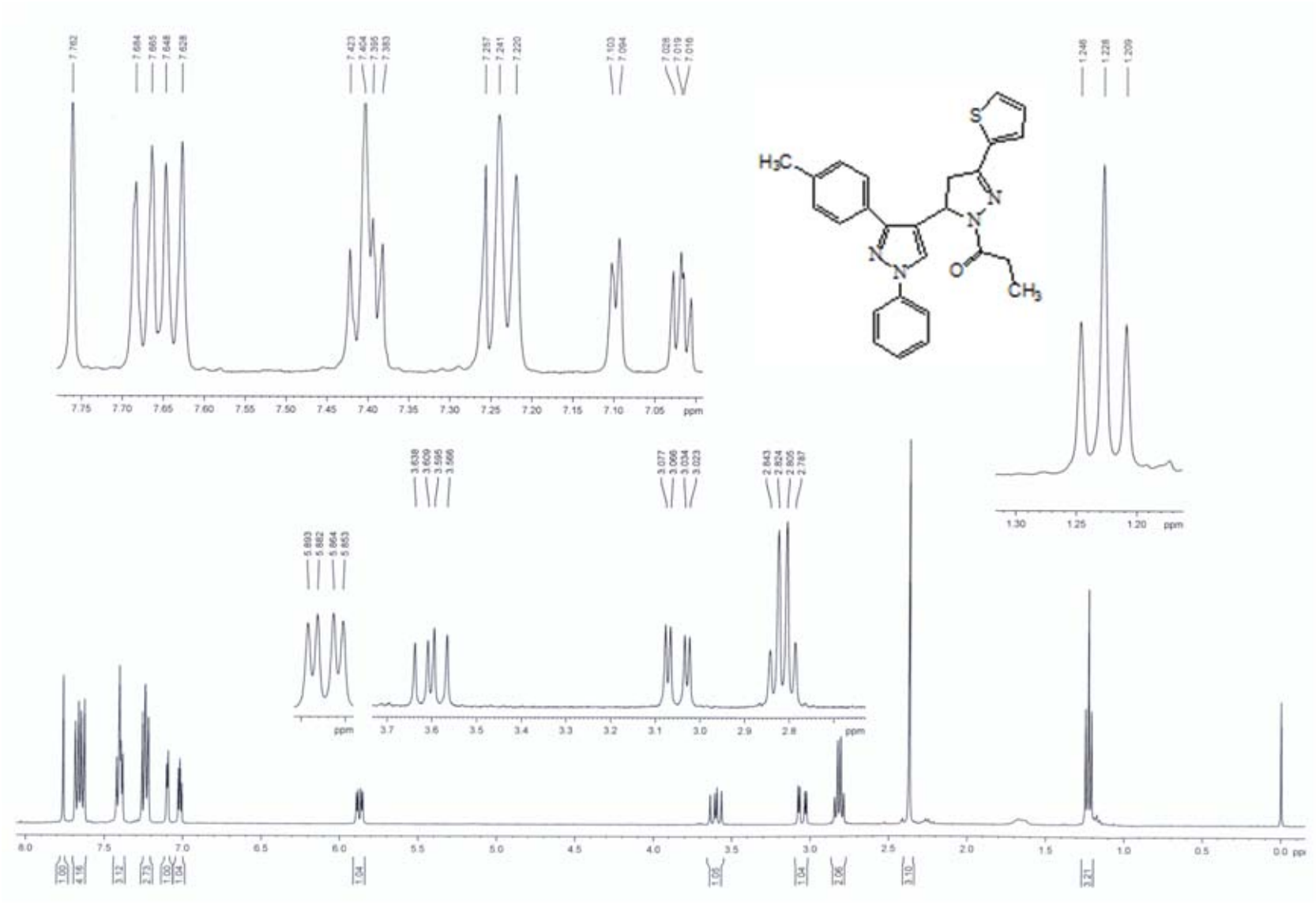

Figure 14: ^{1}H NMR spectrum of compound **IIb** in $CDCl_3$

1-(3-phenyl-5-(1-phenyl-3-p-tolyl-1*H*-pyrazol-4-yl)-4,5-dihydropyrazol-1-yl)propan-1-one (IIIb)

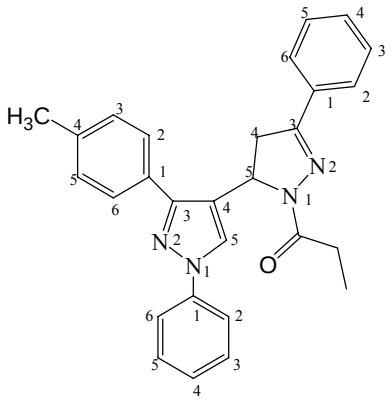

IR (nujol) cm^{-1}: 1647 (C=O); 1594 (C=N).

^{1}H NMR ($CDCl_3$/ CCl_4): δ (ppm) ; 1.25 (t, 3H, J= 7.5 Hz, C<u>H</u>$_3$-CH_2), 2.38 (s, 3H, tolyl-CH_3), 2.86 (q, 2H, J= 7.5 Hz, CH_3C<u>H</u>$_2$), 3.08 (dd, 1H, J=4.4 Hz, pyrazoline-C_4 H), 3.58 (dd, 1H, J=11.6 Hz, pyrazoline-C_4 H), 5.86- 5.90 (dd, 1H, J=4.4,11.6 Hz, pyrazoline-C_5 H), 7.23 (t, 3H, phenyl-$C_{3,4,5}$H), 7.35-7.45 (m, 5H, N_1-phenyl-H), 7.62-7.70 (m, 6H, phenyl-$C_{2,6}$H, p-tolyl-$C_{2,3,5,6}$H), 7.76 (s, 1H, pyrazole-C_5H). Anal. Calcd for $C_{28}H_{26}N_4O$: C, 77.39; H, 6.03; N, 12.89. Found C, **77.21**; H, **5.87**; N, **12.78**.

The IR spectrum of compound **IIIb** is given in figure **15**. Characterstic band attributed to C=O stretching vibration was observed at 1647 cm^{-1}. The band occurred at a low frequency as it is amidic group.

The ^{1}H NMR of compound **IIIb** is shown in figure **16**. Peaks that confirm presence of propanoyl protons were observed as described for compound **IIb**. The two doublet of doublets (integrated for one proton each) at 3.08 ppm and 3.58 ppm, attributed to two pyrazoline-C_4 H and the doublet of doublets that was observed at 5.88 ppm, integrated for

one proton and attributed to pyrazoline-C_5-H confirmed formation of the pyrazoline ring. Two multiplet peaks at 7.35-7.45 ppm and 7.62-7.70 ppm integrated for five and six protons respectively are attributed to the N_1-phenyl-H and phenyl-$C_{2,6}$H, p-tolyl-$C_{2,3,5,6}$-H respectively. The characteristic singlet peak integrated for one proton at 7.76 ppm is attributed to pyrazole-C_5 H.

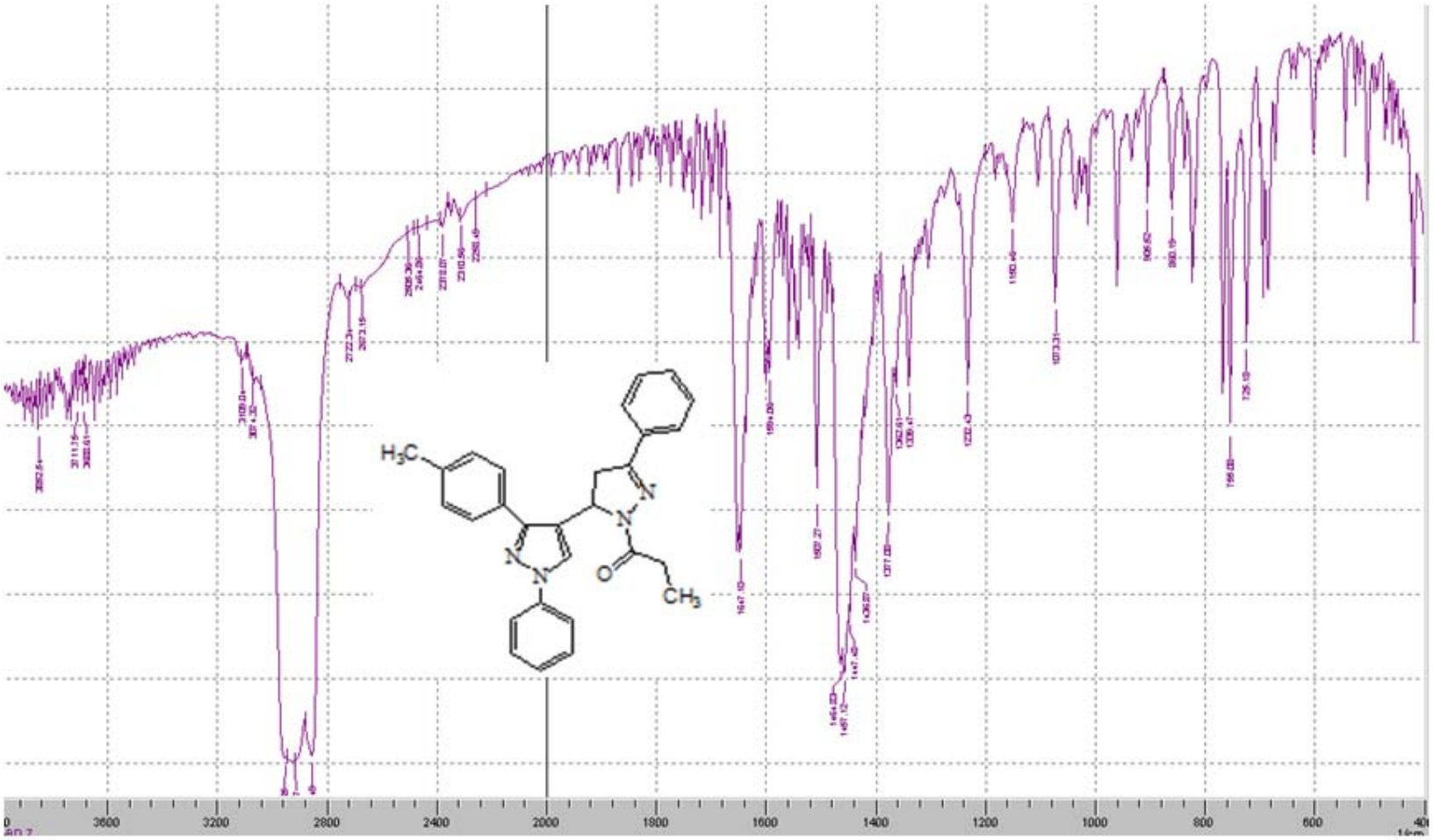

Figure 15: IR spectrum of compound **IIIb** in nujol

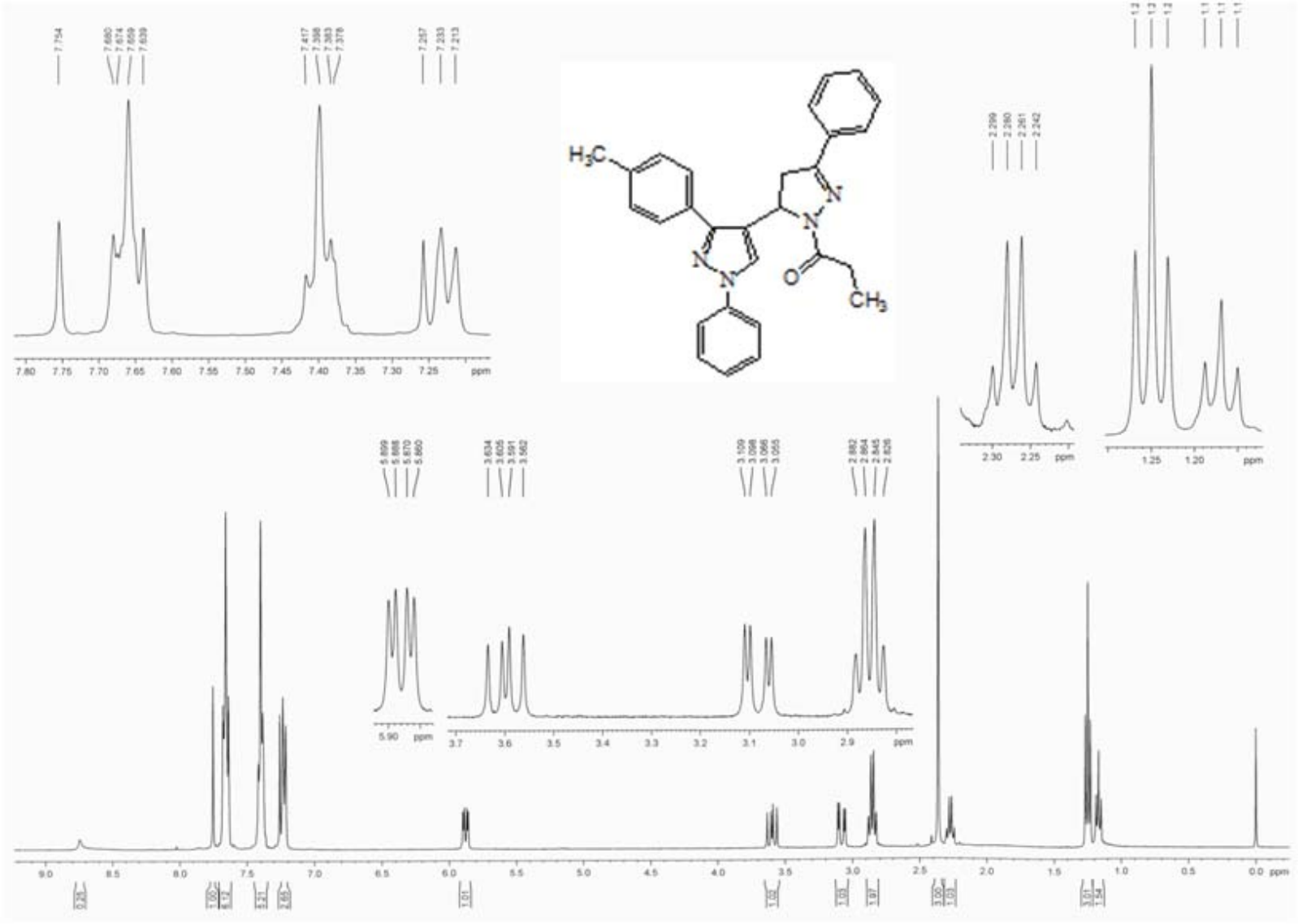

Figure 16: ^{1}H NMR spectrum of compound **IIIb** in $CDCl_3$

1-phenyl-4-(3-(thiophen-2-yl)-4,5-dihydro-1*H*-pyrazol-5-yl)-3-p-tolyl-1*H*-pyrazole (IIc)

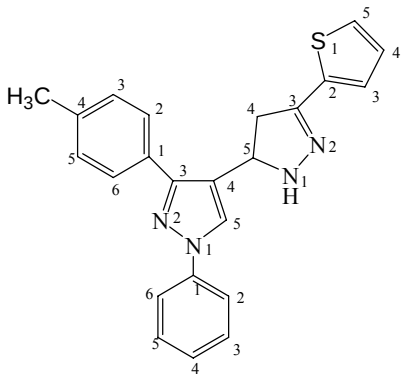

IR (nujol) cm^{-1}: 3300 (N-H);1500 (C=N).

^1H NMR ($CDCl_3$/ CCl_4): δ (ppm); 2.45 (s, 3H, phenyl-CH_3), 3.10 (dd, 1H, J=10.18 Hz, pyrazoline-C_4 H), 3.50 (dd, 1H, J= 8.94 Hz, pyrazoline-C_4 H), 5.17 (t, 1H, pyrazoline-C_5 H), 7.06 (d, 1H, J=5.05 Hz, thiophene-C_5H), 7.12 (d, 1H, J=4.68 Hz, thiophene-C_3H), 7.27-7.50 (m, 6H, N_1-phenyl-H, thiophene-C_4H), 7.61 (d, 2H, J=8.11 Hz, p-tolyl-$C_{2,6}$H), 7.74 (d, 2H, J=7.6 Hz, p- tolyl $C_{2,6}$-H), 8.05 (s, 1H, pyrazole-C_5H). Anal. Calcd for $C_{23}H_{20}N_4S$: C, 71.87; H, 5.24; N, 14.57. Found C, **72.06**; H, **5.57**; N, **14.34**.

The IR spectrum of compound **IIc** is given in figure **17**. No Characteristic band attributed to C=O stretching vibration was observed. The presence of strong band at 3300 cm^{-1} corresponding to NH stretching vibration and absence of the starting ketonic band around 1636 cm^{-1} confirmed formation of the target compound.

The ^1H NMR of compound **IIc** is shown in figure **18**. The two doublet of doublets (integrated for one proton each) at 3.10 ppm and 3.50 ppm are attributed to pyrazoline-C_4 H. The peak for pyrazoline-C_5 H appeared as triplet at 5.17 ppm. Characteristic singlet integrated for one proton and attributed to pyrazole-C_5 H is observed at 8.05 ppm.

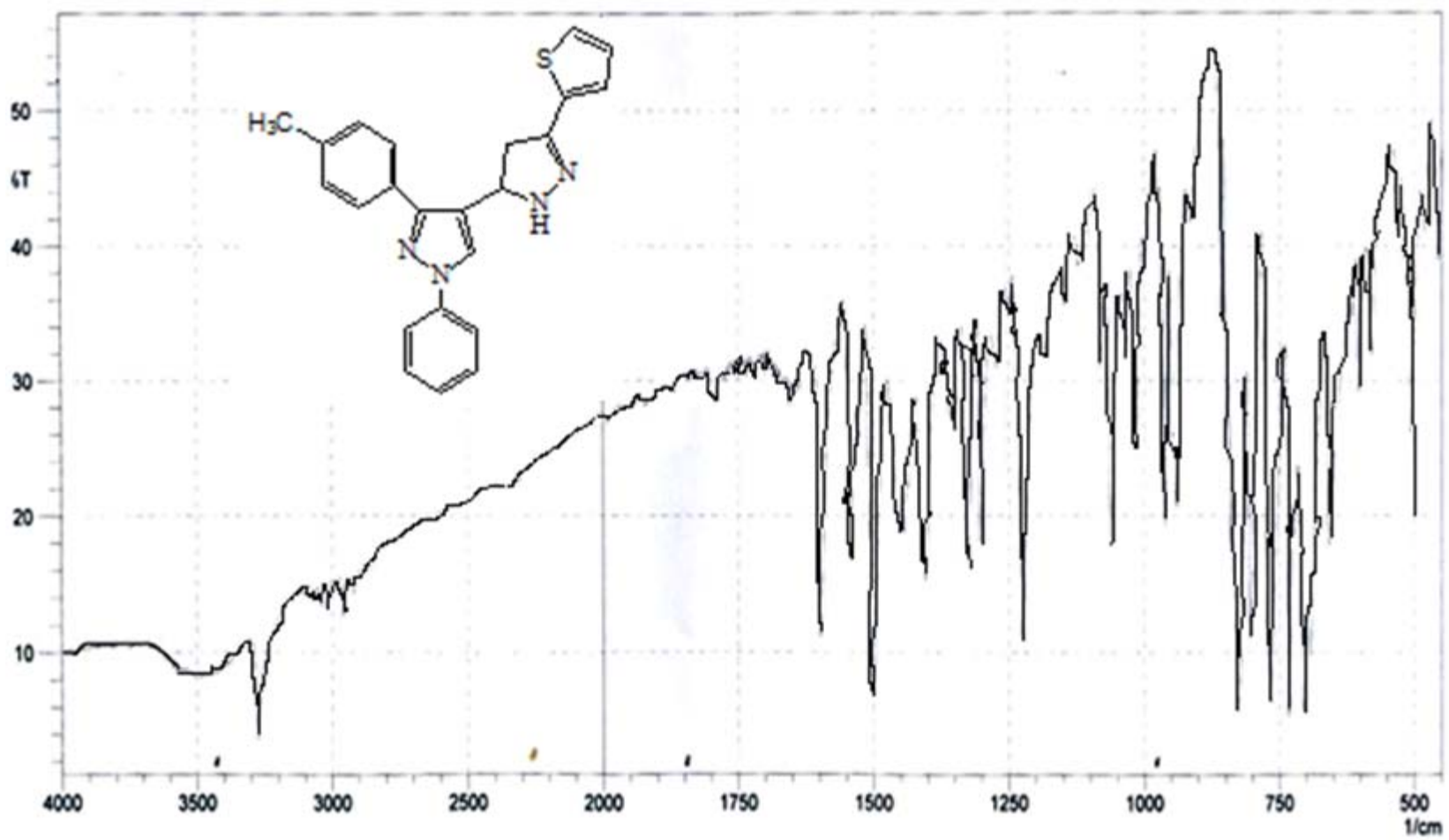

Figure 17: IR spectrum of compound **IIc** in nujol.

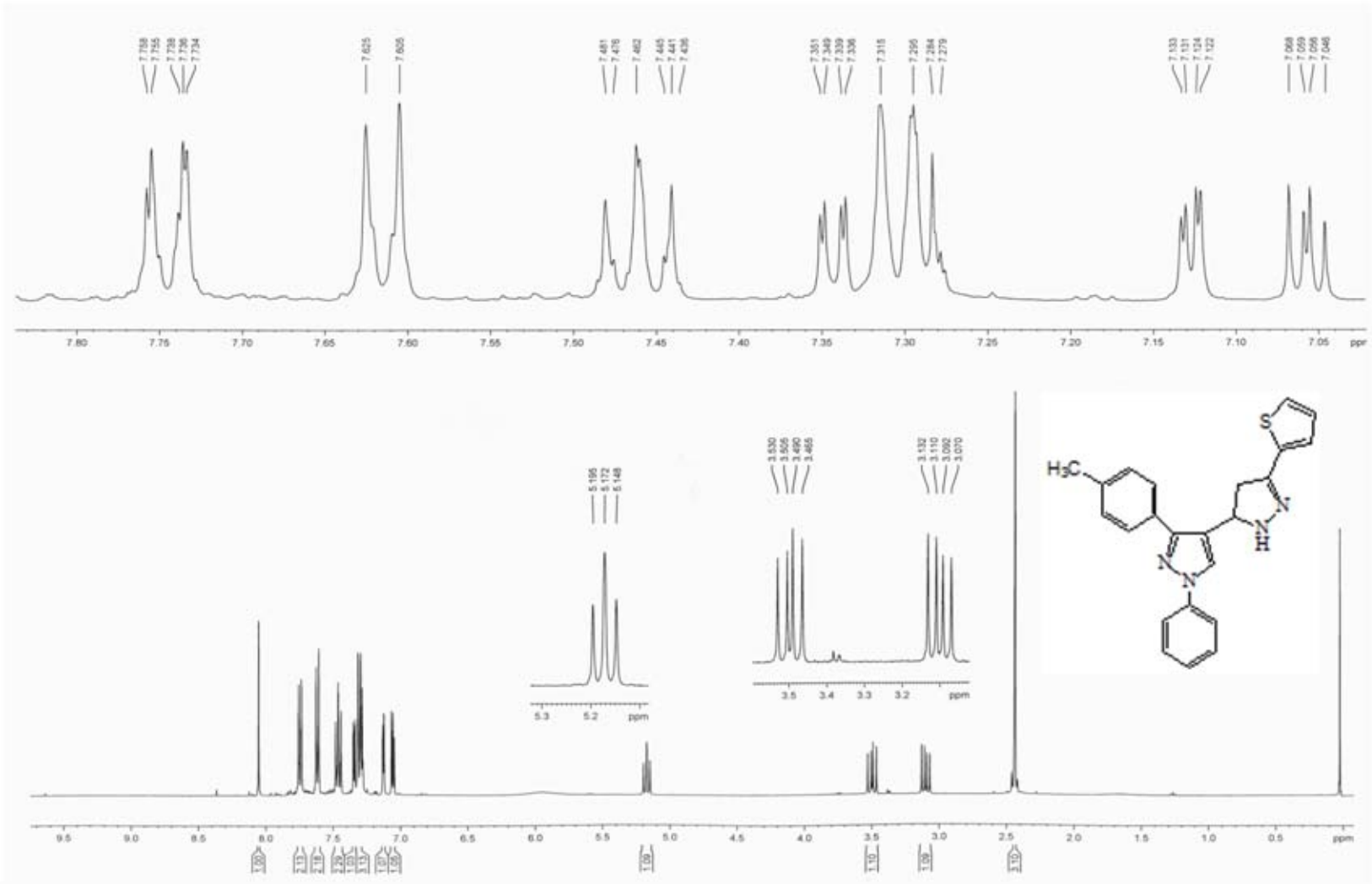

Figure 18: ^{1}H NMR spectrum of compound **IIc** in $CDCl_3$

4.4 Biological assays

4.4.1 *In vivo* antimalarial activity

The synthesized compounds **II**, **III**, **IIa**, **IIIa**, **IIb**, **IIIb** and **IIc** were evaluated for their *in vivo* antimalarial activity using *P. berghei* infected mice at a dose level of 48.46 μmol/kg/day chloroquine phosphate and the solvent were used as positive and negative control, respectively (Table 2).

The antimalarial activity results revealed that all the synthesized compounds have lower activity than the standard drug chloroquine sulphate at the dose level of evaluation. Compounds **IIc** and **IIIb** showed the highest % suppression, 63.40% and 45.52%, respectively. Compound **II** showed the lowest antimalarial activity with % suppression of only 6.78%.

The phenyl derivatives, i.e. compounds **III**, **IIIa**, and **IIIb** showed better antimalarial activity than their respective thienyl derivatives, compounds **II**, **IIa**, and **IIb**.

Table 2: Antimalarial activities for the synthesized compounds at a dose of 48.4 µmol/kg

Test compound	Dose (µmol/Kg)	%parasitemia*	% suppression	Mean survival time (Days)*
II	48.46	46.71±0.25	6.78	5.9±0.21
III	48.46	31.57±0.49	36.99	7.6±0.13
IIa	48.46	40.16±0.18	19.86	6.7±0.85
IIIa	48.46	29.96±0.73	40.21	6.9±0.54
IIb	48.46	33.82±2.9	32.51	7.4±0.38
IIIb	48.46	27.30±0.35	**45.52**	9.2±0.50
IIc	48.46	18.34±0.56	**63.40**	10.2±0.46
Chloroquine phosphate	48.46	0	100	ND
NC**		50.11±0.13	0	5.3±0.53

*Values are Mean ± SD, P<0.05, **NC: Negative control, **ND**: No death recorded over the experimental period.

4.4.2 *In vitro* antipromastigote activity

The antipromastigote assay of the synthesized compounds was carried out according to the method described in the experimental part. The results obtained were analyzed and IC_{50} for each test compound was calculated using Graph pad prism software (Table 3).

The result revealed that all of the synthesized compounds except compound **IIb** possess better antileishmanial activity than the standard drug miltefosine which has IC_{50} value of 3.1911. However, all of synthesized compounds except for compounds **III** and **IIIb** exhibited lower antileishmanial activity compared to the standard amphotericin B deoxycholate. Compound **IIIb**, the phenyl pyrazoline with propanoyl side chain, is found to be the most active (IC_{50}= 0.0112). It was found to be two hundred eigty five fold more active than the standard miltefosine and four fold more active than the standard amphotericin B deoxycholate. The phenyl derivative of both the chalcones and the pyrazolines was proved to have better activity than the corresponding thienyl derivatives. Regarding the thienyl derivatives of the pyrazolines, activity decreased with the increase in the carbon number of aliphatic substitution at pyrazoline N_1 from H to propanoyl group. However, the activity increased with increasing the length of the side chain in the phenyl pyrazolines.

Table 3: Antipromastigote activity (IC_{50}) of the test compounds and reference standards in μg/ml

Test compounds	IC_{50} (μg/ml)	IC_{50} (ng/ml)
II	3.1143	3114.3
III	0.0422	42.2
IIa	2.0730	2073.0
IIIa	1.3076	1307.6
IIb	6.5310	6531.0
IIIb	0.0112	11.2
IIc	0.1673	167.3
Miltefosine	3.1911	3191.1
Amphotericin B Deoxycholate	0.0460	46.0

IC_{50}: values indicate the effective concentration of a compound required to achieve 50 % growth inhibition in μg/ml

5 CONCLUSION

Seven pyrazole derivatives, four thienylpyrazoles and three phenylpyrazoles, were synthesized using aldol condensation and subsequent cyclization reactions. The compounds were produced in a good yield (71.39%-95.20%). The compounds were purified with recrystalization method and their structure was elucidated by elemental microanalysis, IR, and ^{1}H NMR spectroscopy. *In vivo* antimalarial and *in vitro* antileishmanial activity was conducted using four day suppression test and alamar blue reduction method, respectively.

The results for antimalarial activity conducted using *P. berghei* infected mice showed that all the synthesized compounds displayed lower activity than the standard drug chloroquine sulphate with compound **IIc** showing the highest % suppression, 63.40%.

Furthermore, the results for antileishmanial activity revealed that all the synthesized compounds except for compound **IIb** showed better antileishmanial activity than the standard drug miltefosine. But all the synthesized compounds except for compounds **III** and **IIIb** exhibited lower antileishmanial activity compared with the standard amphotericin B deoxycholate. The phenyl pyrazolines showed better antileishmanial activity compared with the thienyl pyrazolines and their activity increased with increase in number of carbons in the side chain. This could be attributed to the associated increase in hydrophobicity of the compounds that increases hydrophobic interaction with the target molecular target site. Compound **IIIb**, phenyl pyrazoline, is found to be the most active (IC_{50}= 0.0112) and two hundred eigty five and four fold more active than the standards miltefosine and amphotericin B deoxycholate respectively. Compound **IIIb** had also shown a better dual acting antimalarial- antileishmanial activity than the rest of the synthesized compounds.

6 RECOMMENDATION

- The antimalarial activity of the compounds wass conducted at a single dose level, hence it should also be carried out at other dose levels to analyze dose-response relationship

- Both antimalarial and antileishmanial activity of the synthesized compounds increased with increase in the length of side chain on the phenyl pyrazolines. Therefore more phenyl pyrazolines of longer side chain has to be synthesized and evaluated.

- Compound **IIIb** has shown a very good antileishmanial activity against *L. donovani.* Therefore the activity should be carried out on the endemic leishmania parasite in Ethiopia, *L. aethiopica.*

- The oral acute toxicity of the most active compound should also be investigated

- Investigation of the mechanism of action and performing docking studies of the most active compound within the active site of relevant receptors is recommended.

- Pyrazole derivatives are shown to have different biological activities; hence evaluation of the synthesized compounds for other biological activities is of importance.

7 REFERENCES

1 WHO, (2009). The World Malaria Report from WHO and UNICEF. World Health Organization, Geneva. 3-9

2 Foster, S. D. (1991). Pricing, distribution, and use of anti-malarial drugs. *Bulletin of the World Health Organization*, **69**: 349–36.

3 Ridley, R.G. (1997). Plasmodium: Drug discovery and development an industrial perspective. *Experimental Parasitology*, **87**: 293–304.

4 Snow, R. W., Guerra, C. A., Noor, A. M., Myint, H. Y. and Hay, S. I. (2005). The global distribution of clinical episodes of *Plasmodium falciparum* malaria. *Nature, 434*: 214–17.

5 Breman, J. G., Alilio, M. S., Mills, A. (2004). Conquering the intolerable burden of malaria. *Am. J. Trop. Med. Hyg*., **71**: 1–15

6 WHO, (2008). The World Malaria Report from WHO and UNICEF. World Health Organization, Geneva. XV

7 WHO, (2010). The World Malaria Report from WHO and UNICEF. World Health Organization, Geneva.

8 Mirjam S., Wondimagegn P. (2006). High prevalence of drug-resistance mutations in *Plasmodium falciparum* and *Plasmodium vivax* in southern Ethiopia. *Malaria j,***5:**54

9 Malaria operational plan (MOP), (2010). President's malaria plan. Ethiopia. 10-11

10 WHO, (2005). Health Action in crises. 1-7.

11 Breman, J. G. (2001). The ears of the hippopotamus: manifestations, determinants

and estimates of the malaria burden. *Am. J. Trop. Med. Hyg*., **64**: 1-11.

12 John, R. and Tabuti, S. (2008). Herbal Medicines used in the treatment of malaria in Budiope country, Uganda. *J Ethno pharmacol,* **116**: 33-42.

13 Federal Ministry of health Ethiopia and WHO, (2007). Entomological Profile of malaria in Ethiopia.3-23.

14 Olliaro P. (2001). Mode of action and mechanisms of resistance for antimalarial drugs. *Pharmacol Ther*, **89:** 207- 219

15 Snehasis J., Jyoti P. (2007). Novel molecular targets for antimalarial chemotherapy. *Int J Antimicro Ag,* **30:** 4–10

16 Noedl H., Schaecher K., Smith B. L., Socheat D. and Fukuda M. M. (2008). "Evidence of artemisinin-resistant malaria in western Cambodia". *N. Engl. J. Med.,* **59** (24): 2619–2620.

17 Mark S. Bailey, Diana N.J. Lockwood,. (2007). Cutaneous leishmaniasis, *Clin Dermatol,* **25:**203-211.

18 Chappuis, F., Sundar, S. and Hailu, A. (2007). Visceral leishmaniasis: what are the needs for diagnosis, treatment and control? *Nat Rev Microbiol.*, **5**: 873–82.

19 Desjeux, P. (1996). Leishmaniasis: public health aspects and control. *Clin Dermatol*, **14:** 417–423.

20 Desjeux, P. (1999). Global control and Leishmania-HIV co-infection. *Clin Dermatol* **17**: 317-25.

21 Reithinger, R., Brooker, S. and Kolaczinski, J. (2007). Visceral leishmaniasis in eastern Africa current status. *Trans. R Soc. Trop. Med. Hyg.,* **101**: 1169–70.

22 Bucheton, B., Kheir, M. M. and El-Safi, S. H. (2002). The interplay between environmental and host factors during an outbreak of visceral leishmaniasis in eastern Sudan. *Microbes Infect,* **4**:1449–57.

23 Mohamed, H. S., Ibrahim, M. E. and Miller, E. N. (2004). SLC11A1 (formerly NRAMP1) and susceptibility to visceral leishmaniasis in The Sudan. *Eur. J. Hum. Genet.* **12**: 66–74.

24 Mengistu G., Akuffo H., Fehniger T. E., Negese Y. and Nilsen R. (1992). Comparison of parasitological and immunological methods in the diagnosis of leishmaniasis in Ethiopia. *Trans. R. Soc. Trop. Med. Hyg.,* **86**: 154-7

25 Gadisa, E., Genetu, A., Kuru, T., Jirata, D., Dagne, K. and Aseffa, A. (2007). Leishmania (Kinetoplastida): species typing with isoenzyme and PCR-RFLP from cutaneous leishmaniasis patients in Ethiopia. *Exp. Parasitol.*, **115**: 339-43.

26 Fernanda G. B., Elaine S. C., Magnum de O. M., Arturene M. L. C., Marisa D. C., Adilson D. da S. (2007). Synthesis and biological evaluation of some 6-substituted purines. *Eur. J. Med. Chem*, **42**:530-537.

27 Sundar S., Chakravarty J. and Rai V. K. (2007). Amphotericin B treatment for Indian visceral leishmaniasis: response to 15 daily versus alternate-day infusions. *Clin. Infect. Dis.,* **45**: 556–61.

28 Mueller, M., Ritmeijer, K., Balasegaram, M., Koummuki, Y., Santana, M. R. and Davidson, R. (2007). Unresponsiveness to AmBisome in some Sudanese patients with kala-azar. *Trans. R. Soc. Trop. Med. Hyg.,* **101**: 19–24.

29 Samir B., Wesam K, Ahmed A. F (2011). Synthesis and antimicrobial activity of

some new 4-hetarylpyrazole and furo[2,3-c]pyrazole derivatives. *Eur. J. Med. Chem*,**46:** 2555-2561

30 Nilesh J. T., Manish P. P. Synthesis, characterization, and antimicrobial evaluation of carbostyril derivatives of 1H-pyrazole (2011). *Saudi Pharmaceutical Journal*, **19:** 75–83

31 Adnan A. Bekhit, Hayam M.A. Ashour, Yasser S. Abdel Ghany, Alaa El-Din A. Bekhit A. B. (2008). Synthesis and biological evaluation of some thiazolyl and thiadiazolyl derivatives of 1H-pyrazole as anti-inflammatory antimicrobial agents. *Eur. J. Med. Chem*, **43:** 456-463

32 Lingaiah N., Jhansi M., Hanmant K. G., Rajashaker B., M. S. Rani, N. J. P. Subhashini (2011). Synthesis and anti-inflammatory activity of some novel 3-phenyl-N-[3-(4-phenylpiperazin-1yl)propyl]-1H-pyrazole-5-carboxamide derivatives. *Bioorg. Med. Chem. Lett.,* **21:** 4138–4140

33 Ramesh B., Chetan M. B. (2011). Novel dihydropyrimidines and its pyrazole derivatives: Synthesis and pharmacological screening. *Eur. J. Med. Chem*, **46:** 1882-1891

34 Marco B., Monica R. L., Giancarlo A. S., Sylvie M., François T., Francesco M (2010). The synthesis and Angiotensin Converting Enzyme (ACE) inhibitory activity of chalcones and their pyrazole derivatives. *Bioorg. Med. Chem. Lett.,* **20:** 1990–1993

35 Hai-Jun C., Yong L., Li-Na W., Qiang S., Jia L., Fa-Jun N (2010). Discovery and structural optimization of pyrazole derivatives as novel inhibitors of Cdc25B. *Bioorg. Med. Chem. Lett.,* **20:** 2876–2879

36 Nesrin G., Samiye Y., Esra K., Umut S., O¨ zen O., Gu¨lberk U., Erdem Y.,

Engin K., Akgu¨l Y., A. A. Bilgina (2007). A new therapeutic approach in Alzheimer disease: Some novel pyrazole derivatives as dual MAO-B inhibitors and antiinflammatory analgesics. *Bioorg. Med. Chem.,* **15:** 5775–5786

37 Mohamed A.Z, Gamal E. A. Abuo-Rahma , Alaa A. H. (2009). Synthesis of novel pyrazole derivatives and evaluation of their antidepressant and anticonvulsant activities. *Eur. J. Med. Chem*, **44:** 3480–3487

38 Guiping O., Zhuo C., Xue-Jian C., Bao-An S., Pinaki S. B., Song Y., Lin-Hong J., Wei X., De-Yu H., Song Z. (2008). Synthesis and antiviral activity of novel pyrazole derivatives containing oxime esters group. *Bioorg. Med. Chem.,* **16:** 9699–9707

39 Ramaiyan M., Ramaiyan V., Shanmugam M., Perumal Y., Dharmarajan S. (2010). Pyrazole derivatives from azines of substituted phenacyl aryl/cyclohexyl sulfides and their antimycobacterial activity. *Bioorg. Med. Chem. Lett.,* **20:** 6920–6924

40 Daniele C., Alessandro De L., Marco R., Beatrice B., Fabrizio M., Matteo M., Sibilla S., Rita M., Lorenza C., Maurizio B. (2008). Synthesis, biological evaluation and SAR study of novel pyrazole analogues as inhibitors of Mycobacterium tuberculosis. *Bioorg. Med. Chem.,***16:** 8587–8591

41 Alice M. R., Adriana O. G., Karen S. C., Antônio C. C. , Gérzia M.C., Marilene M., Leonor L. L., Veronica F. A. (2006). Synthesis and leishmanicidal activities of 1-(4-X-phenyl)-N′-[(4-Y-phenyl)methylene]-1H-pyrazole-4-carbohydrazides. *Eur. J. Med. Chem*, **41:** 80–87

42 Naresh S., Anu A., Sanjay B. K., Nishi, Neena G., Suman G., Prem M. S. Chauhan (2006). Synthesis of 2,4,6-trisubstituted pyrimidine and triazine heterocycles as antileishmanial agents. *Bioorg. Med. Chem.,***14:** 7706–7715

43 Sanjay B. K., Kumkum S., Purib S. K., Prem M. S. Chauhan (2005). Synthesis of 2-[3,5-substituted pyrazol-1-yl]-4,6-trisubstituted triazine derivatives as antimalarial agents. *Bioorg. Med. Chem. Lett.,* **15:** 4957–4960

44 Wilson C., Cleber A. C., Helio G. B., Marcos A. P. Martins, Nilo Z., Marcus V. N. de Souza, Isabela O. Freitas, Rodrigo P. P. Soaresa and Antoniana U. K. (2006). Antimalarial activity of 4-(5-trifluoromethyl-1H-pyrazol-1-yl)-chloroquine analogues. *Bioorg. Med. Chem. Lett.,***16:** 649–653

45 Tizita T. (2010). Synthesis and biological screening of some pyrazoline derivatives as antileishmanial and anti-malarial agents. MSc thesis, Addis Ababa University, Addis Ababa.

46 Parvin K., Sunil K., Khalid H., Ashwani K. (2011). An efficient synthesis of pyrazole chalcones under solvent free conditions at room temperature. *Chinese Chem Lett,* **22:** 37–40

47 Zeba N. S., Mohammed M., Anis Ahmad, Asad U. Khan (2011). Thermal solvent-free synthesis of novel pyrazolyl chalcones and pyrazolines as potential antimicrobial agents. *Bioorg. Med. Chem. Lett.,* **21:** 2860–2865

48 Ju, Y. and Varma, R. S. (2006). Aqueous N-hetrocyclization of primary amines and hydrazines. *J Org Chem*, **71:** 135-141.

49 Singh, P., Negi, J.S., Pant, G.J., Rawat, M.S.M and Asha, B. (2009). Synthesis and Characterization of a Novel 2-Pyrazoline. http://www.mdpi.com/1422-8599/2009/3/M614/pdf pp 1-4, (Accessed on 23.07.2010)

50 Tomilov, Y.V., Guseva, E.V., Volchkov, N.V. and Shulishoy, E.V. (2001). Reactions of diazoalkanes with unsaturated compounds. *Russ Chem b+,* **50:** 2113- 2120.

51 Alex, K., Tillack, A., Schwarz, N. and Beller, M (2008). Zinc catalyzed synthesis of pyrazolines and pyrazoles via hydrohydrazination. *Org Lett,* **10:** 2377- 2379.

52 Tariku, Y., Hymete, A., Hailu, A. and Rohloff, J. (2010). Constituents, Antileishmanial Activity and Toxicity Profile of Volatile Oil from Berries of Croton macrostachyus. *Nat Prod Commun,* **5:** 975-980.

53 Seifert, K., Escobar, P. and Croft, S. L. (2010). In vitro activity of anti-leishmanial drugs against Leishmania donovani is host cell dependent. *J Antimicrob Chemoth,* **10:** 1-4.

54 Foroumadi, A., Pournourmohammadi, S., Soltani, F., Asgharian-Rezaee, M., Dabiri, S., Kharazmi, A. and Shafiee, A. (2005). Synthesis and in vitro leishmanicidal activity of 2-(5-nitro-2-furyl) and 2-(5-nitro-2-thienyl)-5-substituted-1, 3, 4-thiadiazoles. *Bioorg. Med. Chem. Lett.,* **15:** 1983-1985.

55 David, A., Philip, J., Simon, L., Reto, B. and Reto, B. and Solomon, N. (2004). Antimalarial drug discovery: efficacy models for compound screening in vivo and in vitro protocols. http://www.mmv.org/IMG/pdf/screeningpdf_pp1-9, (Accessed on 03.11.10).

56 Kalra, B.S., Chawla, S., Gupta, P. and Valecha, N. (2006). Screening of antimalarial drugs. *Indian J Pharmacol,* **38:** 5- 12.

57 Peters W. and Robinson B. L. (1999). *Parasitic infection models: Handbook of animal models of infection. Acad. Press.,* London: pp 757–773.

58 Dominguez, J., Leon, C., Rodrigues, J., Neira, G. D., Gut, J. and Rosenthal, P. J. (2009). Synthesis of chlorovinyl sulfones as structural analogs of chalcones and their antiplasmodial activities. *Eur. J. Med. Chem*, **44:** 1457–1462.

59 Yang, M., Arai, C., Md, A. B., Lu, J., Ge, G., Pudhom, K., Takasu, K., Kasai, K., Kaiser, M., Brun, R., Yardley, V., Itoh, I. and Ihara, M. (2010). Fluorinated Rhodacyanine (SJL-01) Possessing High Efficacy for Visceral Leishmaniasis. *J med chem,* **53:** 368-373.

60 Al- Nasiry, S., Geusens, N., Hanssens, M., Luyten, C. and Pijnenborg, R. (2007). The use of Alamar Blue assay for quantitative analysis of viability, migration and invasion of choriocarcinoma cells. *Hum Reprod,* **25:** 1-6.

61 Judith M., Dietmar S. (2001). A simple colorimetric method to screen drug cytotoxicity against leishmania using the dye Alamar blue®. *Parasitol. Int.,* **48:** 265-269.

62 Orly S and Charles L. J. (2008). Rapid fluorescent assay for screening drugs on Leishmania amastigotes. *J. Microb. Methods,* **75:** 196–200.

63 Nakayama, G. R., Caton, M. C., Nova, M. P. and Parandoosh, Z. (1997). Assessment of the Alamar Blue assay for cellular growth and viability in vitro. *J Immunol Methods,* **204:** 205–208.